



ChemComm

Promoting Proton Coupled Electron Transfer in Redox Catalysts through Molecular Design

Journal:	<i>ChemComm</i>
Manuscript ID	CC-FEA-07-2019-005139.R1
Article Type:	Feature Article

SCHOLARONE™
Manuscripts

ARTICLE

Promoting Proton Coupled Electron Transfer in Redox Catalysts through Molecular Design

Zachary Thammavongsy,^a Ian P. Mercer,^a and Jenny Y. Yang^{*a}

Received 00th January 20xx,
Accepted 00th January 20xx

DOI: 10.1039/x0xx00000x

Most bond-forming and -breaking redox reactions require the concomitant transfer of protons. Unassisted proton movement can result in kinetic and thermodynamic barriers that inhibit the rate of these reactions, leading to slow and/or inefficient catalysis. These barriers can be circumvented by effective proton management through molecular design. Different strategies for managing proton movement are discussed with examples from biological and synthetic systems. As proton management is particularly important in redox reactions for chemical fuel generation and utilization, the focus will be on catalysts for H-H and O-O bond formation and cleavage. However, we expect the approaches discussed herein will be general to most multi-electron, multi-proton reactions.

Introduction

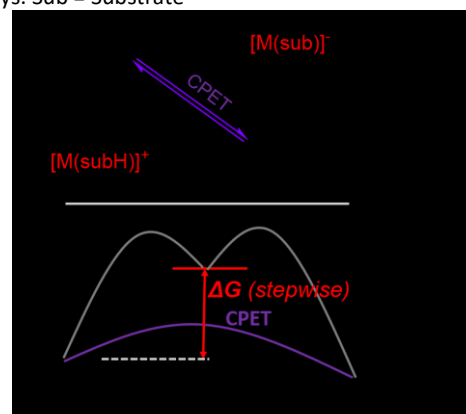
Energy efficient and fast catalysis requires minimizing the energies of intermediates and transition state barriers. For many redox reactions, the addition or removal of protons results in significant energetic obstacles. The issue of proton management is particularly acute in multi-electron and multi-proton processes of fuel-forming and utilization reactions. Catalysts for many reactions relevant to energy storage have been optimized in biological systems; after all, redox catalysis is central to energy transduction in nature. For example, metalloenzymes have evolved several strategies for employing secondary interactions to orchestrate proton transfer. This mini-review will discuss key structural elements for proton management in synthetic redox catalysts and provide relevant parallels to enzymatic systems.

Proton management most commonly includes concerted proton-electron transfer, where the electron and proton move in a single kinetic step. This step is often called CPET¹ but is also referred to as CEP (concerted electron transfer-protonation/deprotonation)² or EPT (electron-proton transfer).³ The biological significance,⁴ theoretical underpinning,^{3b, 5} and experimental validation^{1-2, 5e, 6} of concerted proton-electron transfer have been well documented. The following discussion will focus on its relevance to bond-making and -breaking electron transfer reactions involving protons. The thermodynamics of net proton and electron transfer can be depicted by a square scheme, which is used to describe the oxidation/deprotonation (or net H atom removal) of a metal bound substrate at the top of Scheme 1. The horizontal and vertical axis describe proton and electron transfer, respectively. As a general rule, oxidation of a complex,

M(subH), will result in a more acidic product, [M(subH)]⁺, or pK_{a1} will be greater than pK_{a2}. Similarly, proton removal will result in a more facile oxidation, so E°₂ will be less than E°₁. These trends have been borne out by studies of many organic and inorganic complexes,^{6k, 7} and are also chemically intuitive. It is easier to remove a proton from a cationic species; likewise, it is easier to oxidize an anionic species.

The stepwise electron transfer-proton transfer (ET-PT) pathway must generate [M(subH)]⁺, and the proton transfer-electron transfer (PT-ET) pathway must generate [M(sub)]⁻ (Scheme 1). The energetic cost of accessing either intermediate is determined by the difference in pK_{a1} and pK_{a2}, or E°₁ and E°₂, (ΔpK_a or ΔE°, respectively). Because of the conserved nature of the square scheme, these must be equivalent (−(ΔpK_a)RT = −(ΔE°)F, where R is the universal gas constant, T is the temperature, and F is Faraday's constant).⁸ A larger change in pK_a (ΔpK_a) and reduction potentials (ΔE°) along the stepwise reaction coordinates requires generating even higher energy intermediates. From a chemical standpoint, it is not surprising

Scheme 1. (Top) Square scheme illustrating the thermodynamic parameters for stepwise vs concerted electron-proton transfer and (bottom) corresponding energy landscape for the different pathways. Sub = Substrate



^a Department of Chemistry, University of California, Irvine, 92697, United States
Electronic Supplementary Information (ESI) available: [details of any supplementary information available should be included here]. See DOI: 10.1039/x0xx00000x

that accessing a highly acidic or oxidizing intermediate would be energetically unfavourable. The alternative route, shown as the purple diagonal on the top of Scheme 1, represents concerted proton-electron transfer (CPET). By coupling proton and electron transfer, the two high energy intermediates in red can be circumvented. Processes with greater ΔpK_a or ΔE° values indicate a larger range of conditions in which the concerted path is energetically favourable. Concerted proton transfer is expected to shift the electron transfer potentials to milder values compared to an ET-PT mechanism.

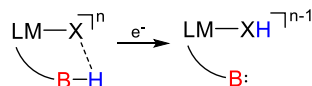
Despite the thermodynamic advantage of concerted proton-electron transfer, significant kinetic barriers exist in the absence of accessible pathways for proton movement. Concerted transfer is highly dependent on the overlap integral for the proton vibrational wave functions between the reactant and product. Maximizing the overlap integral requires decreasing the equilibrium donor-acceptor distances through positioning and/or using molecular thermal motions to increase conformational sampling.^{5a, 9} A suitable proton coordinate can be established by pre-organized proximal association or hydrogen bonding interactions (Scheme 2A).^{6e, 6h, 10} The pK_a of the proton acceptor or donor should also be matched to facilitate concerted movement with the redox event. For example, if oxidation results in an increase in acidity of the substrate, the proton acceptor should have a slightly lower pK_a than the substrate prior to oxidation (pK_{a1} in Scheme 1). The pK_a match can also impact hydrogen-bonding interaction between the donor and acceptor, which in turn can affect the kinetics of CPET.¹¹

Even in the absence of concerted proton-electron transfer (CPET), interactions in the secondary coordination sphere provide additional advantages for redox catalysis. The secondary coordination sphere can manage proton inventory for convenient intramolecular delivery or removal to the redox-active site (Scheme 2B). Outer-sphere functionalities not directly involved in proton movement can establish hydrogen bonded networks for proton shuttling. Local protonation sites or proton relays to external bases can also facilitate sequential proton transfer upon electron transfer, levelling the reduction potential of subsequent electron transfer events (Scheme 2C). As a result, multiple electron transfer events can occur within a narrow potential window. Catalyst pre-protonation can shift reduction potentials positive or facilitate a fast protonation step upon electron transfer, which would lead to lower overpotentials for reductive catalysis. The broader term proton coupled electron transfer (PCET) encompasses these stepwise events.^{5a} Proximal or distal hydrogen bond donors or acceptors can also assist in substrate orientation at critical bond-making or -breaking steps.

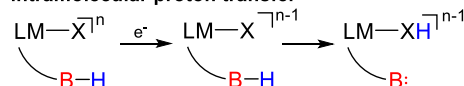
A few common themes emerge in the design of catalysts for effective proton management. Among these are the importance of both the positioning and the pK_a/pK_b of secondary interactions. Positioning is critical in the equilibrium catalyst structure and for potential dynamic behaviour. Rigid pendant acids/bases provide more control between their distance to the substrate, but flexibility allows for distance optimization through conformational sampling. However,

Scheme 2. Various functions for secondary interactions in proton management shown as reductions (oxidations would follow the microscopic reverse). A. CPET, where the e^- and H^+ transfer occur in a single kinetic step, B. stepwise transfer facilitated by a proximal proton source, and C. redox-levelling through sequential electron-proton transfer. Secondary interactions can also assist in orienting substrate (not shown).

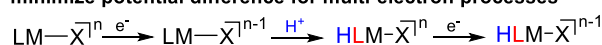
A. Concerted Proton-Electron Transfer (CPET)



B. Stepwise electron-proton transfer facilitated by intramolecular proton transfer



C. Redox-levelling with proton-responsive ligands can minimize potential difference for multi-electron processes



Bronsted bases are often also good ligands, and too much flexibility can result in coordination to the metal. In some cases, pendant base coordination is not an issue as ligands can labilize under catalytic conditions to serve a secondary function in proton management. The pK_a/pK_b of the pendant base is also important as it should be matched to their proton donor or acceptor function. The pK_a/pK_b value also defines whether they will function as an acid or base under catalytic conditions.

Modifying the secondary coordination sphere will also impact the steric profile of the reaction site and the ligand field, which may also impact catalytic activity. Steric contributions to catalysis can be isolated by synthesizing analogues with functionalities that have similar steric footprints but cannot accept or donate a proton or hydrogen-bond (i.e. replacing carboxylic acid analogues with their ester analogue, or alcohols with methyl ethers). Changes in the active site electronic structure through addition of secondary functionalities can also affect catalytic activity, either by altering the mechanism or by modifying the driving force (changing the onset potential) for catalysis. In the latter case, shifting the reduction potential to more extreme values (and thus a greater overpotential) will often result in higher rates due to the more favourable free energy, or driving force, for the reaction. Examining linear free energy relationships between overpotential and rate can help distinguish whether improvements in catalytic activity are due to electronic and steric contributions or proton management from secondary interactions.¹²

The design elements and considerations for proton management described herein are applicable to any redox reaction. However, this article will focus on molecular catalysts for H-H and O-O bond formation and cleavage with a focus on examples that utilize secondary interactions. References to more comprehensive reviews for each reaction will be included in each section. We note a prior review on molecular electrocatalysts that utilize PCET for these reactions along with CO_2 and N_2 reduction.¹³ In line with the guidelines for a feature

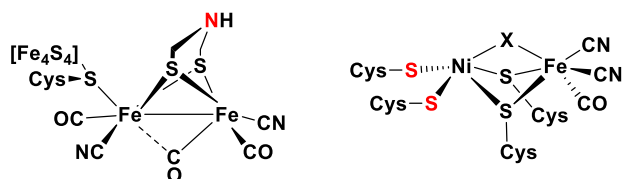
article, examples from the corresponding author's own research will be highlighted.

Hydrogen Evolution and Oxidation

In nature, the hydrogenase enzymes catalyse the production and oxidation of hydrogen. There are three major classes, the [NiFe], [FeFe], and [Fe] hydrogenases.¹⁴ The activity of multiple variants has been characterized electrochemically.¹⁵ Although most variants demonstrate reversible electrocatalytic activity, they typically demonstrate bias towards either H⁺ reduction or H₂ oxidation.¹⁶

The active site structures of the [FeFe] and [NiFe] hydrogenase are shown in Chart 1 and specific features will be discussed in the context of functional synthetic mimics. The [FeFe] hydrogenase utilizes a pendant amine bridge to facilitate proton movement,¹⁷ and both active sites contain thiolate ligands that are proposed to function as a proton reservoir during the catalytic cycle¹⁸ (although in the case of [NiFe] hydrogenase, a proximal cysteine may also be involved).¹⁹ These two motifs: 1) a fixed proton relay or 2) employment of a protonatable ligand bound to the metal have been mimicked in synthetic catalysts and will be discussed.²⁰ A more comprehensive review of electrocatalysts for these reactions is also available.²¹

Chart 1. Active sites for the (left) [FeFe]-hydrogenase and the (right) [NiFe]-hydrogenase where X is an oxide, sulfur, hydroperoxide, or a hydroxide.



A Family of Reversible Catalysts for H⁺/H₂ Conversion

A defining trait of the hydrogenase enzymes is their reversible catalytic activity. By the principle of microscopic reversibility, a reversible catalyst must operate near the thermodynamic potential. One of the most well-known classes of synthetic catalysts capable of reversible catalysis at high rates is the nickel bis(diphosphine) [Ni(P₂N₂)₂]²⁺ complexes initially developed by D. DuBois and M. R. DuBois.²² Although the mechanistic understanding and activity of this class of catalysts have been substantially improved by a large team of co-workers through experiment and theory (including co-author Yang), the initial framework was conceived to promote concerted proton-electron transfer step to circumvent a high energy intermediate and its associated kinetic barrier.

Early work on the family of [Ni(P₂N₂)₂]²⁺ complexes was devised for the reverse reaction, hydrogen oxidation. Since low overpotential catalysts must be reversible, catalyst design can benefit from optimizing the reaction from either direction. Early studies by DuBois and co-workers found the first step in a potential hydrogen oxidation reaction (heterolytic cleavage of H₂) to be exergonic with [Ni(depp)₂]²⁺ (Figure 1, right) and Et₃N to form the hydride [HNi(depp)₂]²⁺ and Et₃NH⁺, respectively.²³

However, this step was slow under electrocatalytic conditions and operated at a significant overpotential. A thermodynamic analysis of the proposed catalytic cycle was used to construct a free energy landscape (Figure 1a-b). It quickly became apparent that while most steps in the proposed catalytic cycle had minimal changes in free energy as desired, one step stood out – oxidation of the [HNi(depp)₂]⁺ to [HNi(depp)₂]²⁺ (a Ni(III) hydride). The high energy (by 13 kcal/mol) of [HNi(depp)₂]²⁺ is evident by its very acidic pK_a value of -3.2. Although the Ni(III)H would certainly be deprotonated under catalytic conditions by an exogenous Et₃N base, stepwise oxidation of [HNi(depp)₂]⁺ to [HNi(depp)₂]²⁺ requires a much higher potential, contributing to the large overpotential. Since concerted proton-electron transfer is facilitated by a local proton donor or acceptor, a proton acceptor was installed by amending the depp ligand to incorporate an amine base for intramolecular deprotonation of the metal hydride. Like depp, the new ligand PNP (Figure 1, in complex **2**) forms a six-membered ring upon coordination to the metal. In the 'boat' conformation, the amine base of complex **2** is positioned for proton-exchange with the metal hydride. The facility to which the pendant amine exchanges protons with the metal was ascertained through rapid incorporation (<5 min) of deuterium from D₂O to [HNi(PNP)₂]⁺. In contrast, only partial incorporation of deuterium was observed in the equivalent experiment using [HNi(depp)₂]⁺ (<10% after 48 hours).²⁴ Additional studies verified that the pendant amine proton exchanged with the metal hydride proton at rates of at least 10⁴ s⁻¹ at room temperature.²⁵ The experimental evidence reveals the importance of correct *positioning* and pK_a of the pendant base to facilitate concerted proton-electron transfer. The new, more energy efficient pathway enabled by the pendant amine was evident by its electrocatalytic activity. The overpotential of hydrogen oxidation by [Ni(PNP)₂]²⁺ was reduced by 0.65 V. Although the energetic efficiency was significantly improved, the rate of catalysis was still comparable to [HNi(depp)₂]²⁺ since the pendant base is only appropriately positioned in the higher energy 'boat' conformation. Addition of a second six-membered ring ensured the pendant base was favourably positioned in the ground state conformation, leading to the more familiar [Ni(P₂N₂)₂]²⁺ variant shown at the bottom of Figure 1. (Modifying the P substituents from Et in [HNi(PNP)₂]⁺ to Cy in [HNi(P₂N₂)₂]⁺ decreases the latter's hydricity, which disfavors H₂ oxidation. This effect is compensated by increasing the basicity of the pendant amine by changing its substituent from Me to Ph so that both compounds have negative free energies for H₂ addition/cleavage).²⁶

Subsequent studies provided additional information on the importance of the position and quantity of pendant bases on reactivity. An experimental study on heterolytic H₂ cleavage found the lowest energy pathway to initiate catalysis utilizes two positioned bases instead of one.²⁷ A subsequent computational study found the calculated equilibrium distance between the Ni and the N base to be 3.25 Å, which is too far for easy proton transfer. However, thermal fluctuations permit more appropriate distances for concerted PCET.²⁸ These results prompted the computational study of nickel catalysts with more flexible pendant amines, but they were found to have even

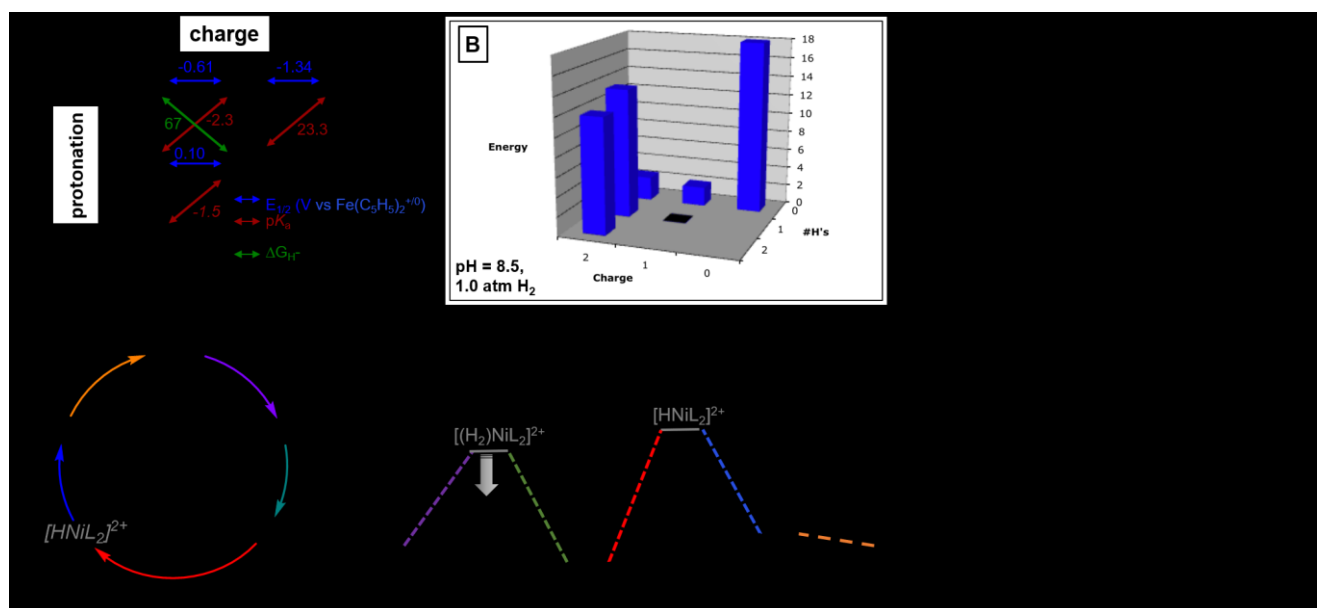


Figure 1. (A) Square scheme outlining the thermodynamic properties of potential intermediates in an $2\text{H}^+/\text{H}_2$ catalytic cycle, (B) relative energies of each species in the square scheme at pH 8.5 under 1.0 atm H_2 , (C) proposed catalytic cycle for H_2 oxidation, (D) relative energies of each intermediate in the proposed catalytic cycle from (C) using data from (B) illustrating the high energy required to access a Ni(III) hydride which can be circumvented through coupled proton-electron transfer. The extent of CPET is dependent on the operating potential. (Box, right) Three generations of catalysts derived through successive thermodynamic and kinetic analysis. (A) and (B) adapted with permission from *Chem. Soc. Rev.*, 2009, **38**, 62-72. Copyright 2009 Royal Society of Chemistry

greater equilibrium distances, underscoring the importance of positioning and rigidity with thermal flexibility in second-sphere proton acceptors.²⁸⁻²⁹

The molecular dynamics and isomers of the complex have also been investigated.³⁰ These studies led to the incorporation of amino acid functionalities in the tertiary or outer coordination sphere for control of the local solvation or proton transfer network, leading to even faster catalysis at lower overpotentials.^{22b, 31} The ligand architecture and related variants have also been used to promote hydrogen evolution catalysis for cobalt catalysts.³² Although advances have been made in catalyst optimization,³³ the basic design stemmed from installing an appropriately positioned base that would facilitate the proton movement of a particularly (energetically) troublesome proton-electron transfer step.

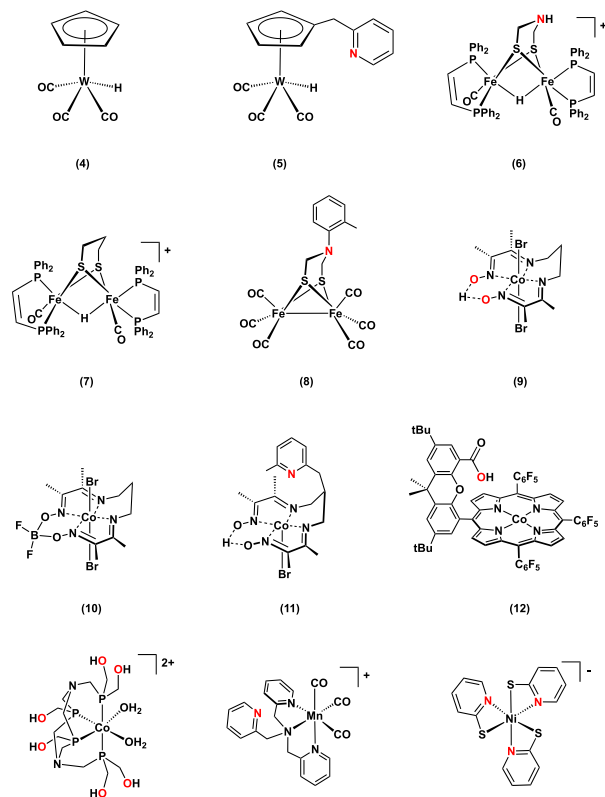
More recently, Hammarström and co-workers have demonstrated how synthetic design can promote intramolecular proton transfer to metal hydrides. An early study demonstrated oxidation of a tungsten hydride could proceed through a concerted mechanism with an exogenous base (Chart 2, 4).³⁴ However, this route was slow as metal hydrides are weak hydrogen bond donors and pre-organization with the proton acceptor was minimal. Subsequent incorporation of a pendant pyridine base in the secondary coordination sphere accelerated the concerted pathway by a factor of 10^4 , illustrating the importance of intramolecular proton pathways (Chart 2, 5).³⁵

Hydrogen Evolution Catalysis with Secondary Coordination Sphere Proton Relays

Rauchfuss and co-workers have extensively reported on structural and functional mimics of hydrogenase active sites.³⁶ We highlight one example that resembles the [FeFe] hydrogenase active site, shown in Chart 2 (6).³⁷ This complex contains a rigid pendant amine base in the secondary coordination sphere and is an electrocatalyst for proton reduction in organic solvents. The study presents several interesting mechanistic insights into the role of the amine bridge. Strong acids such as HBF_4 can protonate the amine into the ammonium species, which is stabilized by the BF_4^- anion. The ammonium species can be protonated a second time to generate a terminal iron hydride. The precise positioning of the amine bridge was highlighted with a remarkable crystallographic study of the doubly protonated species. The structure depicts a small distance between the hydride and the ammonium proton, suggesting a hydrogen bond. The close hydride/proton interaction provides a snapshot of a species that likely precedes hydrogen bond formation or cleavage. The study also reported the congener without the pendant base (Chart 2, 7). Both analogues have some electrocatalytic activity for proton reduction. However, the lack of an amine bridge results in significantly larger overpotentials and slower rates. Complex 6 and 7 are almost indistinguishable spectroscopically, indicating similar electronic effects between the two ligands. Thus, the dramatic changes in activity are attributed to the presence of the pendant amine instead of the modified electronic or thermodynamic properties between the two complexes.

The structural rearrangements necessary for a bridgehead N to function as a pendant base in diiron hydrogenase mimics

Chart 2. **4** and **5** illustrate how CPET can be facilitated by an intramolecular H⁺ acceptor. **6–15** are molecular catalysts for H⁺ reduction; some demonstrate enhanced activity with proximal H⁺ donors (shown in red).



have been investigated by Darensbourg and coworkers.³⁸ A subsequent study by Darensbourg, Dey, and co-workers found the nitrogen pendant base and local hydrogen bonding were also important for parallel O₂ reduction to H₂O (Chart 2, **6**). As a result, the complexes could reduce protons to H₂ in the presence of O₂ without significant oxidative degradation.³⁹ Dey and co-workers also reported an [FeFe]-hydrogenase mimic that is catalytically active in acidic H₂O (pH < 3).⁴⁰

The family of cobalt macrocycles commonly called cobaloximes has been extensively studied for their high electrocatalytic activity towards H₂ evolution. The experimental work⁴¹ has been complemented and informed by theoretical studies.⁴² For this article, we focus on a few aspects of ligand design that we find pertinent to facilitating proton transfer in hydrogen evolution. A comprehensive understanding of the proposed mechanisms and activity of cobaloximes can be found in recent reviews.^{41–42}

A common variant of cobaloximes contains two O-BF₂-O bridges in the macrocycle. Replacement of the O-BF₂-O bridges by O-H-O provides a second-sphere proton relay, but the resulting complex is less stable under acidic conditions.⁴³ Artero and co-workers reformulated the macrocycle as a hybrid propyl-dioxime ligand with one O-H-O bridge (Chart 2, **9**), leading to a stable cobalt complex.⁴⁴ Electrocatalytic studies on **9** uncovered positive shifts in the operating potential when stronger acids were used, whereas the analogous BF₂ derivative

exhibited minimal changes (Chart 2, **10**). The authors suggested that protonation of the oxime ligands led to more facile reduction for entry into the catalytic cycle. The protonated oxime may also facilitate catalysis by maintaining a local proton inventory or allowing intramolecular H-H bond formation. Aqueous studies with this complex also exhibited a positive Nernstian shift of 60 mV with each decreasing pH unit, indicating a one-electron, one-proton process.⁴⁵ A computational study provided additional insight into the ligand protonation and provided estimated redox and pK_a values.⁴⁶ The study indicated intramolecular proton transfer from the ligand to the metal was exergonic but accompanied by a large energy barrier. However, the authors noted nearby solvent molecules could assist in the proton transfer.^{46a}

Incorporating a dangling pendant base has also been investigated for the cobaloxime system. Early studies reported an appended pyridine coordinated to the metal to form a five-coordinate 'ariat-type' structure,⁴⁷ which was also investigated for photocatalytic hydrogen evolution activity.⁴⁸ Peters, Miller, and co-workers hypothesized installing a methyl functionality next to the pyridine would prevent coordination, which was validated by the solid-state structure (Chart 2, **11**).⁴⁹ The combined experimental and computational studies indicated the pendant pyridine served as an intramolecular proton shuttle for the formation of the metal hydride intermediate. The computational results indicated the presence of the proton relay decoupled the relationship between reduction potential and rate of hydride formation, resulting in faster catalysis without an increase in overpotential.⁴⁹

Rigid pillars containing a pendant functionality have been installed on several types of tetradentate square planar macrocycles to mediate proton movement for hydrogen and oxygen catalysis. This 'hangman' motif was explored by Nocera and co-workers in the cobalt complex shown in Chart 2, compound **12**.⁵⁰ H-H bond formation is proposed to proceed through the protonation of a Co(II)H intermediate. An initial study noted the importance of the second-sphere carboxylic acid group in promoting intramolecular proton transfer to generate Co(II)H, which reduced the overpotential of H₂ evolution.^{50a} A significant increase in the rate of protonation to form the Co(II)H species was observed.^{50b} Based on the second order rate constants of Co(II)H formation with external benzoic acid (analogues lacking the intramolecular proton donor), the proton relay provides an effective acid concentration of >3000 M. The use of an intramolecular proton donor to facilitate formation of the metal hydride intermediate preceding H₂ evolution is reminiscent of the [Ni(P₂N₂)₂]²⁺ class of compounds discussed earlier. A complete energy landscape for catalysis in both the weak and strong acid regime was also reported, providing insight into the energetic advantages of the CPET steps in the catalytic cycle.^{50c} Similar benefits in electrocatalytic activity from the 'hangman' functionality were also found in the nickel congener.^{50c, 51} Detailed spectroscopic and computational studies point to a PT-ET mechanism, instead of the ET-PT mechanism favoured by the corresponding cobalt complex. Interestingly, the product of the one-electron reduction of the Ni(I) complex is more accurately described as a Ni(I) porphyrin

radical. Thus, the Ni complex harnesses ligand-based orbitals to stabilize the reduced species.

More flexible pendant bases have also been used to facilitate proton transfer. A cobalt complex with a multi-hydroxy-functionalized tetraphosphine ligand reported by Sun and co-workers catalyses the electrochemical reduction of neutral water with under 100 mV overpotential (Chart 2, **13**).⁵² A subsequent computational study found the hydroxy functionalities contribute to a hydrogen bonding network in the secondary coordination sphere, permitting concerted proton-electron transfer for metal hydride formation, as well as directing subsequent protonation for H₂ evolution.⁵³

In most coordination complexes, tris(2-pyridylmethyl)amine is a tetradentate ligand. However, Richeson and co-workers demonstrated the coordination of tris(2-pyridylmethyl)amine to fac-Mn(CO)₃ leads to a dangling pyridine ligand (Chart 2, **14**).⁵⁴ Complex **14** is an active electrocatalyst for the reduction of H₂O in CH₃CN. Density functional theory indicates the uncoordinated pyridine functions as a proton relay for hydride formation. The tertiary amine in the ligand then protonates further in the catalytic cycle to deliver the second proton to the Mn hydride.

An interesting example reported by Eisenberg and co-workers is a six-coordinate (and thus saturated) nickel complex that is proposed to dechelate upon protonation to form an open coordination site and a pendant base (Chart 2, **15**).⁵⁵ The complex has three bidentate pyridine thiolate ligands in the resting state. The first protonation occurs at a pyridine nitrogen, resulting in dissociation from the metal. The newly exposed coordination site at the metal can be reduced and protonated to form a nickel hydride. The protonated pyridine then delivers its proton to evolve H₂.

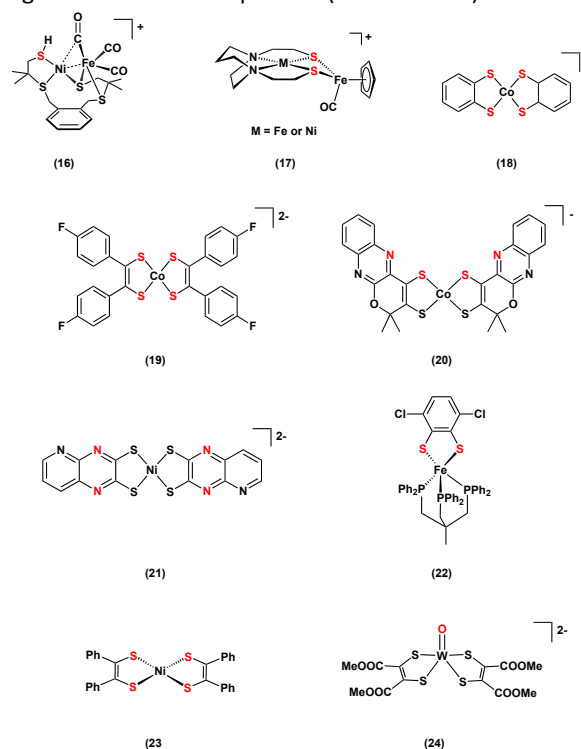
Hydrogen Evolution Catalysis using S-Ligands as a Potential Proton Reservoir

As mentioned above, the [FeFe]-hydrogenase utilizes a pendant base to coordinate proton movement into the primary coordination sphere. There is evidence the [FeFe]- and [NiFe]-hydrogenases may also utilize a protonated cysteinate in the primary coordination sphere as a proton reservoir.^{14, 18c-e, 56} There is an interesting parallel between the proposed 'proton-active' role of thiolate ligands in the hydrogenase enzyme, the molecular systems described below, and the highly active heterogeneous catalyst MoS₂.⁵⁷ The latter served as inspiration for the molecular analogue [(Py₅Me₂)MoS₂]²⁺,⁵⁸ with the role of the S₂ moiety explored using quantum mechanical methods.⁵⁹

A synthetic heterobimetallic NiFe complex reported by Lubitz and co-workers provided evidence of thiolate protonation (Chart 3, **16**).⁶⁰ Although the protonated thiolate was bound to the Ni, spectroscopic and DFT studies describe how protonation impacts the electronic structure of the adjacent iron site. Complex **16** is also an active electrocatalyst for proton reduction in organic solvents.

Darensbourg, Hall, and co-workers explored the electronic structure and protonation properties of a series of hydrogenase bimetallic complexes bridged with thiolate ligands (Chart 3, **17**). Mechanistic studies indicate reduction-induced hemilability of the metallothiolate ligands upon protonation, which can then

Chart 3. Molecular catalysts for H⁺ reduction with thiolate ligands that are H⁺ responsive (shown in red).



serve as a proton donor to form H₂ at a metal-based hydride.⁶¹ The authors noted the positioning and distance of the proton donor are key for H₂ evolution. A related paper examined the importance of sequential proton-electron delivery in mediating catalytic potentials.⁶²

Stepwise double protonation of the thiolate ligand has been cited as a key mechanistic feature in photo- and electrocatalytic proton reduction by cobalt dithiolene complexes (Chart 3, **18**).⁶³ The proton can then undergo intramolecular transfer from the ligand to the metal to form a cobalt hydride intermediate, which then couples with a second proton on the ligand to form the H–H bond. A theoretical study estimated the pK_a of the protonated form of **18** and related complexes. The study found the protonation under catalytic conditions contributed to a lower catalytic overpotential. When ligand protonation was possible, the positive charge levelled the reduction potential, contributing to catalysis at lower overpotentials.⁶⁴

Catalytic proton reduction by a related series of cobalt dithiolene complexes reported by Head-Gordon, Tilley, and co-workers also invoked the S atom of the thiolate ligand as a proton acceptor (Chart 3, **19**).⁶⁵ Experimental and computational studies indicate that protonation of the reduced cobalt complex first occurs on the metal to form a cobalt hydride intermediate. Upon the second reduction event, protonation forms a bound SH ligand near the hydride prior to facile H₂ evolution.

Li, Fontecave, and co-workers have explored proton reduction using cobalt complexes with molybdopterin-like ligands (Chart 3, **20**).⁶⁶ Molybdopterin is a bidentate S-donor ligand commonly found in W/Mo-containing redox

metalloenzymes. The molybdopterin-like ligands on the Co center contain multiple protonation sites. Not only can the S-ligands be protonated, each ligand also has a basic N-site. The multiple protonation sites engender several possible mechanistic pathways for sequential or coupled proton and electron transfer. Akin to the dithiolene systems previously mentioned, the intermediate prior to H₂ evolution is a cobalt hydride with a protonated thiolate ligand. However, the presence of the N-protonation site on the molybdopterin-like ligands results in a more anodic reduction potential, lowering the overpotential for catalysis.

Sakai and co-workers also reported a nickel-based dithiolene aqueous electrocatalyst with N atom protonation sites on the ligand (Chart 3, **21**).⁶⁷ Like the prior example with the molybdopterin-like ligands, they are not positioned for intramolecular proton transfer. However, a Pourbaix diagram of the different possible species at varying pH and potential indicates that protonation under catalytic conditions is likely, resulting in an increase in reduction potential and reducing the overall electrocatalytic overpotential. The authors note that protonation on the S-donor ligands is unlikely; instead, the N atoms are the most basic site.

An iron-based electrocatalyst with a triphosphine and dithiolene ligand was reported (Chart 3, **22**).⁶⁸ The proposed mechanism suggests that upon reduction, the most basic site on the complex is the S-ligand donor. After a second reduction, the proton migrates to the metal to form an iron hydride, which is directly protonated to form H₂.

Electrocatalytic proton reduction activity was reported for a nickel bis(aryldithiolene) complex (Chart 3, **23**).⁶⁹ In contrast to the proposed mechanisms for the related cobalt complexes, experimental and computational data for this catalyst support a mechanism in which the S-ligands are protonated twice and no metal hydride is ever formed. The doubly-protonated ligand is due to the higher nucleophilicity (basicity) of the S-ligands. The reductive events are ligand-based and the nickel maintains its divalent oxidation state throughout the catalytic cycle.

A tungsten oxide dithiolene catalyst (Chart 3, **24**) reported by Fontecave and co-workers follows the same theme of utilizing a ligand donor atom as the proton reservoir.⁷⁰ However, the S-ligands are innocent in this mechanism. Instead, protonation is believed to occur on the oxo ligand. Subsequent protonation at the W results in the hydride, followed by intramolecular H-H bond formation.

Hydrogen Oxidation Catalysis with Positioned Proton Acceptors

Although electrocatalytic H₂ oxidation is a key reaction for fuel cell utilization, few examples of molecular catalysts have been reported.

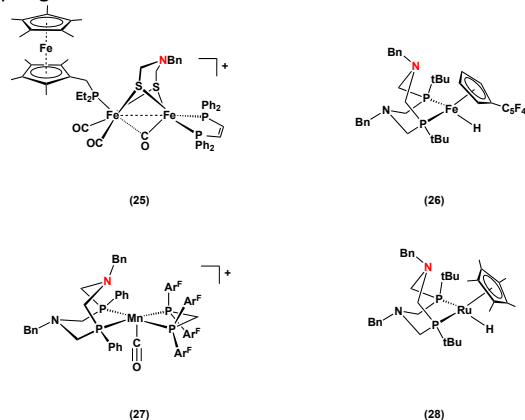
Rauchfuss and co-workers reported facile hydrogen oxidation by a synthetic mimic of the active site of the [FeFe] hydrogenase enzyme (Chart 4, **25**).⁷¹ Under 2 atm of H₂ at room temperature, the diiron complex quantitatively reacts over a few hours to cleave the H-H bond and form the protonated amine and a diferrous iron hydride complex. H₂ binding of the complex is rate-determining. The role of the pendant amine in H-H bond cleavage was clarified when compared to the

analogue without a pendant base, which is unreactive to H₂ under the same conditions.

Several variants of the [Ni(P₂N₂)₂]²⁺ family of compounds have been optimized for H₂ oxidation. The overall thermodynamic bias for H₂ oxidation can be tuned by modifying the substituents on the P donors (which adjust the hydride acceptor strength of the metal) or the pendant N (which modifies its pK_a).⁷² The importance of matching the pK_a of the base and appropriate positioning was demonstrated by the variable energetic pathways accessible in the catalytic cycle. Facile deprotonation prior to oxidation of the H₂ addition species led to a decrease in overpotential by 0.38 V.⁷³ Additional studies elaborated on specific solvent and electrolyte effects,⁷⁴ or the outer coordination sphere on the rate of catalysis.⁷⁵

The P₂N₂ ligand and related analogues have also been used in the development of iron (Chart 4, **26**),⁷⁶ manganese (Chart 4, **27**),⁷⁷ and ruthenium (Chart 4, **28**)⁷⁸ based hydrogen oxidation catalysts. Similar to H₂ activation by the nickel analogues, the bases promote heterolytic cleavage to form a hydride and protonated base in the secondary coordination sphere.

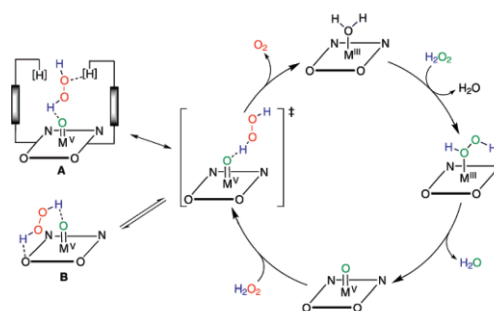
Chart 4. Molecular electrocatalysts for H₂ oxidation; proximal H⁺ accepting functionalities are shown in red.



Proton Relays in O-O Bond Cleavage and Formation

The importance of concerted proton-electron transfer has been long recognized in making and breaking the O-O bond. The intimate details of both processes are of interest for artificial

Scheme 3. Proposed catalytic cycle for H₂O₂ disproportionation by hangman salen complexes. Reprinted with permission from *J. Am. Chem. Soc.*, 2007, **129**, 8192-8198. Copyright 2007 American Chemical Society.



photosynthetic cycles (H_2O oxidation to O_2) and fuel cells (O_2 reduction to H_2O). The disproportionation of H_2O_2 reflects the two-electron variant of both reactions. In nature, cytotoxic H_2O_2 is quenched by catalase enzymes that promote heterolysis of the O-O bond to form a high-valent metal oxo species, which rapidly reacts with a second equivalent of H_2O_2 to form H_2O and O_2 .⁷⁹ Mutagenesis studies on myoglobin validate the importance of distal acid/base residues on O-O bond heterolysis.⁸⁰ A study by Saveant and co-workers also noted the significant thermodynamic and kinetic impact a proximal acid group had on O-O cleavage in organic peroxides.⁸¹

Complexes incorporating a macrocycle in a 'hangman' motif, or with secondary coordination sphere pendant acid/base functionalities, have been used to investigate the impact of proximal acid/base functionalities in O_2 activation.⁸² The same family of complexes were previously described for their electrocatalytic HER activity. In line with these goals, co-author Yang and co-workers constructed a series of 'hangman' Mn(III)Cl Schiff base complexes to explore H_2O_2 activation and catalase activity.⁸³ Stopped-flow spectroscopic studies using a variant with one pendant carboxylic acid confirmed the generation of a high valent Mn(V) oxo intermediate upon reaction with H_2O_2 , which subsequently reacts with a second equivalent of H_2O_2 to form O_2 and H_2O .^{83a} Unlike the proposed kinetic profile for catalase enzymes, formation of the Mn(V) oxo intermediate is not rate-limiting. Instead, positioning of the second H_2O_2 substrate at the Mn(V) oxo center is critical for fast catalysis (Scheme 3, intermediate **A**). Computational studies indicate that in the absence of directing carboxylic acids in the secondary coordination sphere, H_2O_2 could bind to form an unproductive, off-cycle intermediate that is prone to decomposition (Scheme 3, intermediate **B**).⁸⁴

Further insight into the importance of positioning was elucidated using a modified framework that installed two carboxylic acid functionalities at two different distances relative to the metal center (Chart 5, **29** and **31**).^{83b} In both cases, the complexes with pendant carboxylic acids led to significantly higher rates of H_2O_2 dismutation compared to the congeners with an ester functionality or unmodified Mn(salen)Cl with two equivalents of exogeneous benzoic acid. However, the variant with carboxylic acids positioned over the metal center (**31**) had about half the activity. Energy-minimized structures obtained from DFT revealed the carboxylic acids in **31** were positioned sufficiently close to form a hydrogen bond with each other. The intramolecular hydrogen bond decreased the acidity of the carboxylic acid protons, inhibiting the stabilization of incoming substrate. In contrast, the more distant carboxylic acid in **29**

could easily hydrogen bond to position incoming substrate. To further avoid formation of off-cycle intermediate **B** (Scheme 3), the ligand framework was modified to install t-butyl functionalities proximal to the phenoxide ligand (Chart 5, **30** and **32**).^{83c} Addition of these steric blocking groups led to a 3x increase in overall turnover number and a greater than 2x increase in the initial rate constant.

The catalase activity of Mn Schiff base complexes is of broader interest as a therapeutic treatment for minimizing reactive oxygen species (ROS).⁸⁴⁻⁸⁵ These studies illustrate the different ways in which a pendant acid functionality (and hydrogen bond donor) can facilitate O-O bond forming and cleavage events and orient substrate. The experimental and computational studies on the 'hangman' Mn Schiff complexes ultimately led to a 33-fold improvement in catalase activity through systematic molecular design.

H₂O oxidation in Nature and Synthetic Architectures

In nature, the Oxygen Evolving Complex (OEC) in Photosystem II catalyses the oxidation of water to liberate proton and electron equivalents for carbon dioxide reduction. The active site has a Mn_4CaO_5 cluster embedded in an extensive and finely-tuned hydrogen bonded network, which is composed of secondary residues and water molecules.⁸⁶ The importance of these secondary residues is reflected in the diminished activity upon modification or removal.⁸⁷

Secondary interactions have the potential to play multiple roles in H_2O oxidation. Activation of coordinated H_2O is typically the first step to catalytic oxidation. In the OEC, this event is coordinated with proton movement to a local tyrosine (Tyr₂) and histidine (His) pair.⁸⁸ In synthetic systems, the pK_a of metal-bound aqua or hydroxide complexes decrease by at least 6 units upon oxidation. The significant increase in acidity signifies the key role proton-coupling in water oxidation can play in avoiding high energy intermediates.⁸⁹ Facile proton removal also mediates the reduction potential; for example, the OEC performs the four-electron oxidation of water within a narrow 0.3 V range.⁹⁰ Redox leveling has also been observed with sequential, as well as concerted, proton transfer.⁹¹

Secondary sphere hydrogen bonding interactions can also assist in bringing in or orienting substrate, often the second equivalent of H_2O . Two major mechanisms for O-O bond formation have been proposed: the nucleophilic attack of water on an electrophilic metal oxo species or the coupling of two M-O units.⁹² In the former mechanism, a more distant proton acceptor can accelerate O-O bond formation by increasing the nucleophilicity of the second H_2O for reaction to the metal oxo species. Modifying the nucleophilicity of H_2O through concerted proton removal has been referred to as atom-proton transfer (APT).⁹³ Our discussion is focused on examples of the multiple ways in which secondary interactions can promote water oxidation in synthetic systems. More comprehensive reviews of synthetic molecular examples of water oxidation catalysts are also available.^{21, 92, 94}

H₂O Oxidation Facilitated by Intermolecular Pre-organization in Solution. A unique feature of water oxidation is that excess substrate can pre-assemble to form hydrogen bonded networks for concerted proton transfer or shuttling.^{6f} Water or buffer can

Chart 5. Salen hangman complexes used to investigate the catalytic disproportionation of H_2O_2 .

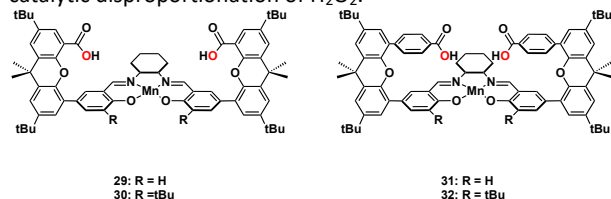
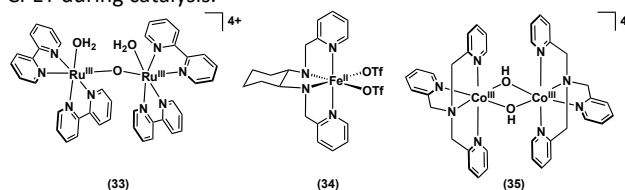


Chart 6. Molecular catalysts for H₂O oxidation proposed to utilize intermolecular hydrogen-bonded networks to manage CPET during catalysis.



also serve as the proton donor or acceptor. As a result, positioned bases on the ligand are not essential for promoting coupled proton transfer. The relationship between reduction potential and proton activity (or Pourbaix diagram) depicts the coupling of proton movement to electron transfer by the Nernst equation. Additionally, these diagrams also reveal the magnitude of intermediate pK_a changes with redox events.

The first well-defined molecular catalyst for water oxidation, the μ -oxo-bridged “blue dimer” diruthenium complex (Chart 6, **33**) described by Meyer and co-workers illustrated strong coupling between proton-electron transfer without an intramolecular base.⁹⁵ The intimate relationship is illustrated in the strong dependence of reduction potential with pH for the aquo/hydroxide/oxo species. Additionally, facile deprotonation enables ‘redox leveling’ to access high oxidation states within a narrow potential range. Parallels in proton management in the mechanism of the blue dimer and the OEC have been described in detail.⁹⁶ Subsequent studies demonstrated that single-site Ru complexes are also competent water oxidation catalysts. These complexes also have a strong reduction potential dependence on proton activity, characteristic of strongly coupled proton-electron transfer in aqueous solution.⁹⁷

A series of iron complexes with multi-dentate N-donor ligands were investigated for water oxidation activity by Lloret-Fillol, Costas, and co-workers using the chemical oxidants cerium ammonium nitrate at pH 1 and sodium periodate at pH 2.⁹⁸ Their study found that two cis open coordination sites were key to catalytic activity (Chart 6, **34**). A subsequent study used experimental and calculated pK_a values, and reduction potentials to generate a thermodynamic square scheme. Based on this data, the authors concluded the high Fe(V) oxidation state necessary for catalysis was only accessible through coupled proton-electron transfer.⁹⁹

A cobalt dimer with photocatalytic water oxidation activity reported by Fukuzumi, Kojima and co-workers (Chart 6, **35**) also described a strong correlation between the first two oxidation events and pH.¹⁰⁰ This relationship was reflected in the measured pK_a values for the first and second deprotonation events of the bis- μ -hydroxide complex to give a putative bis- μ -oxyl Co(III) species proposed to precede the O-O bond formation. DFT calculations indicate the second (proton coupled) oxidation is the rate-determining step.

Meyer and co-workers used [Ru(Mebimpy)(bpy)(OH₂)]²⁺ [where Mebimpy = 2,6-bis(1-methylbenzimidazol-2-yl)pyridine] to explore the impact of different exogenous bases on water

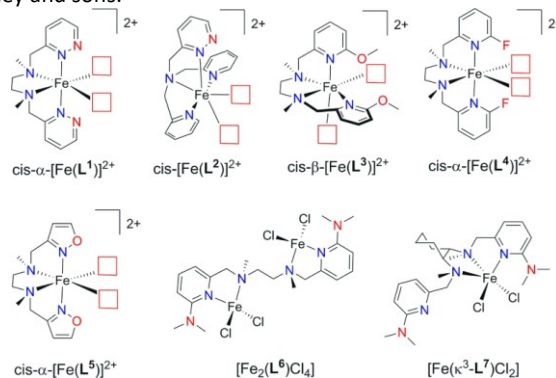
oxidation activity.⁹³ They described the concerted proton transfer from a water molecule with its reaction to a high valent metal oxo to form the O-O bond as a concerted atom-proton transfer (APT). Meyer and co-workers cited a similar mechanism for water oxidation in a Cu catalyst with a triglycylglycine ligand, since the catalytic rate exhibited a strong dependence on the concentration of the buffer bases HPO₄²⁻ and PO₄³⁻ at otherwise fixed pH values.¹⁰¹ The Cu complex also displayed pH dependent reduction potentials consistent with concerted proton transfer. **Synthetic Catalysts for H₂O Oxidation with Proton Shuttles Incorporated into the Secondary Coordination Sphere.**

Co-author Yang and co-workers reported the synthesis of a series of multi-dentate N-donor ligands with pendant proton acceptors in the secondary coordination sphere (Chart 7).¹⁰² The ligands were based on oxidation resistant pyridine and amine frameworks. The corresponding iron complexes were explored for water oxidation using the chemical oxidant, cerium(IV) ammonium nitrate, at low pH. Under these conditions, the pendant bases were likely protonated and thus exhibited no enhanced activity for water oxidation.

A subsequent study focused on the cobalt complex of the dipyridyldiamine ligand with proximal dimethylamine bases (Figure 2).¹⁰³ Solid-state structures of the mono- and di-aqua complexes established the dimethylamines were positioned to form hydrogen bonds with bound water substrate. The pK_a of comparable Co(II) aqua complexes with similar ligands and that of dimethylaniline indicates the pendant base is well-matched to accept an aqua proton upon oxidation to Co(III). Cyclic voltammetry and controlled potential electrolysis revealed electrochemical water oxidation activity whereas the analogue without pendant bases was inactive, underscoring the importance of the local proton acceptors.

Several catalytic and mechanistic studies have been reported on complexes with the ‘hangman’- type architecture. An early study illustrated how a hanging carboxylic group functionality on a xanthene spacer creates a hydrogen bonded ‘pocket’ created over a porphyrin macrocycle.^{82a} A subsequent study with the fluorinated cobalt analogue described the pH-

Chart 7. Iron complexes of a series of ligands incorporating various secondary interactions. Reprinted with permission from *Eur. J. Inorg. Chem.*, 2013, **2013**, 3846-3857. Copyright 2013 John Wiley and sons.



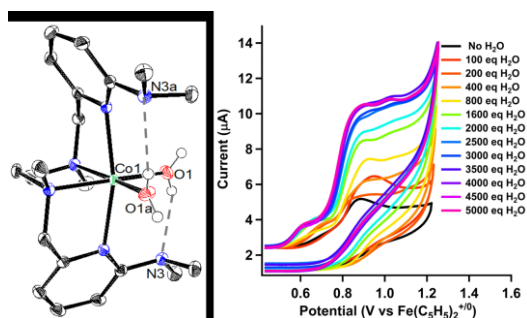


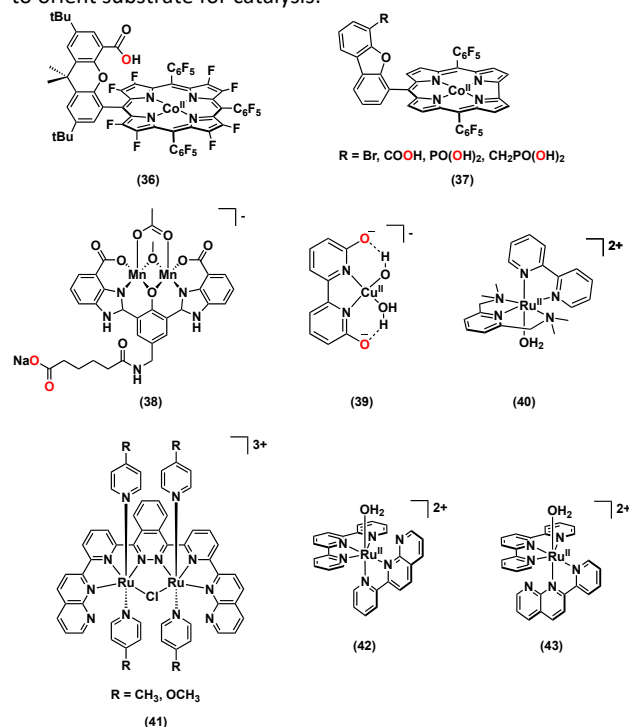
Figure 2. (left) ORTEP of solid-state structure of $[\text{Co}(\text{L}^{\text{DMA}})(\text{H}_2\text{O})_2]^{2+}$ illustrating the hydrogen bonds to the bound aqua ligands. Outer-sphere anions are omitted. (right) Cyclic voltammetry upon titration of water into a solution of $[\text{Co}(\text{L}^{\text{DMA}})(\text{H}_2\text{O})_2]^{2+}$ in acetonitrile illustrating water oxidation activity. Reproduced with permission from *Chem. Sci.*, 2018, 9, 2750-2755 - Published by The Royal Society of Chemistry.

dependent catalytic water oxidation activity of the 'hangman' derivatives, which was greater than the activity of the equivalent macrocycle lacking a distal carboxylic acid (Chart 8, **36**).¹⁰⁴ The authors cited the carboxylic acid's role in pre-organizing the catalytic site as an important contributor to its activity. Two subsequent computational studies shed additional insight into the mechanism of H_2O oxidation. Cramer and co-workers indicated that O-O bond formation was facilitated by the intrinsic electrophilicity of the oxidized species (due to its peripheral fluorination) and concerted proton transfer from the nucleophilic water to the positioned pendant base.¹⁰⁵ Another computational study by Lai, Chen, and co-workers explored a series of high valent metals in this ligand scaffold and found the Co analogue had the most favourable energetics for O-O bond formation.¹⁰⁶ Electrocatalytic water oxidation was also reported for an electron deficient Co-corrole lacking pendant bases.¹⁰⁷ Although the complex has no intramolecular proton acceptors, the reduction potential displays a Nernstian relationship with pH, indicating coupled proton-electron transfer, likely through intermolecular pre-organization in water.

Related 'hangman' corrole complexes using dibenzofuran pillars were reported by Cao and co-workers.¹⁰⁸ The dibenzofuran spacer positions the acid/base functionalities further from the transition metal macrocycle. They found the phosphoric acid derivative was more active for water oxidation than the more acidic carboxylic acid analogue. Insertion of a methylene group between the dibenzofuran and phosphoric acid led to even greater reactivity, underscoring the importance of positioning and pK_a for enhanced activity (Chart 8, **37**). Based on the positioning of the acid/base functionality, the authors suggest it facilitates proton removal from a water substrate to enable nucleophilic attack on a high valent oxo at the metal.

Åkermark and co-workers reported a series of oxygen-bridged dinuclear Mn complexes for water oxidation (Chart 8, **38**).¹⁰⁹ Anionic ligands were used to decrease the reduction potential of the complexes and stabilize higher oxidation states. The ligand backbone was functionalized with various non-rigid

Chart 8. Molecular catalysts for H_2O oxidation that incorporate secondary interactions (shown in red) as either H^+ acceptors or to orient substrate for catalysis.



proton acceptors. Catalytic studies found the highest rates corresponded to the complex with a distal carboxylate group, although no reduction in overpotential was observed. Although the carboxylate is not rigidly positioned, the DFT optimized structure indicates it can hydrogen bond with hydroxide ligands on the Mn atoms, or assist with orienting incoming H_2O .

Electrocatalytic water oxidation activity under alkaline conditions was characterized for Cu complexes of 6,6'-dihydroxy-2,2'-bipyridine (Chart 8, **39**).¹¹⁰ The position of hydroxyl functionalities proximal to the two open coordination sites on the Cu are essential to the low observed overpotential. However, this may be due to its role in mediating proton transfer or by contributing to the redox non-innocence of the ligand, resulting in more facile oxidation. Although calculated reduction potentials and pK_a values indicate possible concerted proton-electron transfer, the authors were unable to characterize the relevant catalytic intermediates.

High water oxidation activity at low overpotentials has been reported by Maayan and co-workers for Mn₁₂ clusters. In the first reported variant, the Mn atoms are bridged by 3,5-dihydroxybenzoic acid.¹¹¹ The authors suggest the hydroxyl substituents contribute to the catalytic activity by assisting with proton or water transfer through hydrogen bonding networks in the secondary coordination sphere. This hypothesis is supported by the improvement of the catalytic rate (by three orders of magnitude), faradaic efficiency of 93%, and low overpotential (74 mV) of the analogue bridged with 3,4,5-trihydroxybenzoic acid, which adds an additional 16 hydroxyl

substituents to the surface of the cluster.¹¹² The authors note that the bridging ligand is expected to be redox-active, which may contribute to the mild oxidation potential of the cluster as well as stabilizing higher oxidation states in the Mn atoms.

The water oxidation catalyst $[\text{Ru}(\text{II})(\text{damp})(\text{bpy})(\text{H}_2\text{O})]^{2+}$ [where damp = 2,6-bis(dimethylamino)pyridine] (Chart 8, **40**) reported by Llobet and coworkers does not have an acid/base functionality in the secondary coordination sphere.¹¹³ However, the DFT optimized structure of the Ru(IV) oxo intermediate illustrates a strong hydrogen bonded network around the oxo ligand.¹¹⁴ The presence of these interactions are supported by the narrow gap (~ 0.14 V) between the first two oxidation events of $[\text{Ru}(\text{II})(\text{damp})(\text{bpy})(\text{H}_2\text{O})]^{2+}$ to generate the oxo. The authors cite the importance of a locally positioned water for proton removal to facilitate nucleophilic attack to form the O-O bond (APT).

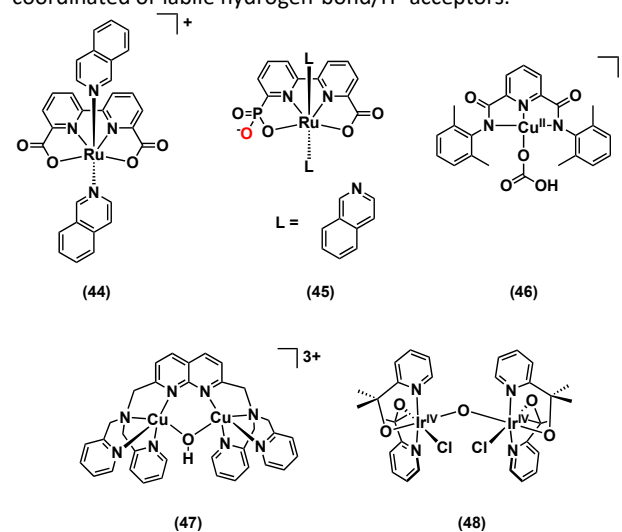
Thummel and co-workers have reported a series of mononuclear and dinuclear Ru polypyridyl complexes with water oxidation activity using Ce(IV) as a chemical oxidant. Several of these complexes contain naphthyridine units, which poise an N-based proton acceptor near an open coordination site (Chart 8, **41**).¹¹⁵ A solid-state structure found the proton acceptor was appropriately positioned to hydrogen bond with a coordinated water molecule.¹¹⁶ A more recent study compared two monomeric isomers with the N-based proton acceptor oriented towards and away from the open coordination site (Chart 8, **42** & **43**).¹¹⁷ Counterintuitively, the latter exhibited much higher activity towards water oxidation. Spectroscopic studies indicated that the proton acceptor was very weakly basic and unprotonated at pH values as low as 0. Thus, the lack of enhanced activity with the proximal base is likely due to an ineffective pK_b value for facilitating concerted proton transfer. Since the pK_a of uncoordinated 1,8-naphthyridine is 3.4 in water, it is clear that coordination of one N-atom to Ru significantly reduces the proton affinity of the other N-atom.

H₂O Oxidation with Coordinated or Labile Hydrogen Bond or Proton Acceptors

Sun and co-workers reported a series of single-site seven-coordinate Ru catalysts with two coordinated carboxylates (Chart 9, **44**).¹¹⁸ A solid-state structure demonstrated a dimer is stabilized through hydrogen bonding with Ru-bound water along with outer-sphere water molecules to comprise a proton network.^{118a} In line with this structure, the first two oxidation-deprotonation events for the Ru(III) aqua complexes to generate the Ru(V) oxo are very rapid. Experimental and computational results indicate O-O bond coupling is the rate-determining step.^{118b, 118c}

A related single-site Ru system was reported by Concepcion and co-workers using a hybrid ligand with both a carboxylate and a phosphonic acid (Chart 9, **45**).¹¹⁹ This complex is among the fastest reported homogeneous catalysts for water oxidation. The ligand design incorporates several key elements for low barrier catalysis, including proton coupled oxidation of the Ru aqua species to generate the high valent Ru oxo and

Chart 9. Molecular catalysts for H₂O oxidation that utilize coordinated or labile hydrogen-bond/H⁺ acceptors.



promotion of the base-assisted atom-proton transfer (APT) pathway to lower the energetic barrier for O-O bond formation.

Lai, Cao, and co-workers described the water oxidation activity of a Cu(II) *N,N'*-2,6-dimethylphenyl-2,6-pyridinedicarboxamate complex (Chart 9, **46**).¹²⁰ They propose that the fourth coordination site for the square planar complex is occupied by a carbonate anion in carbonate buffer solutions. Computational studies indicate the carbonate anion can intramolecularly accept a proton from a bound aqua species to generate a more oxidized intermediate, which can then relay the proton to exogenous buffer.

A dinuclear copper complex has a labile ligand acting as a pendant base (Chart 9, **47**).¹²¹ In the resting state each copper complex is coordinated by four N-donor ligands and are bridged by a hydroxide ligand. Computational analysis suggests a pyridyl ligand dissociates to permit coordination of the first water substrate. The pyridine then acts as a base to mediate successive deprotonation events of the bound water and bridging hydroxide.

Crabtree, Brudvig and co-workers have utilized the asymmetric ligand pyalk (pyalk=2-(2-pyridyl)isopropanoate) in iridium complexes for successful water oxidation catalysis. The ligand is oxidatively resistant, leading to greater catalyst stability. In addition, the ligand is a strong electron donor, which stabilizes higher oxidation states (Chart 9, **48**).¹²² The alkoxy groups can also intramolecularly accept a proton. The basicity of the alkoxy increases with the oxidation state of the metal. The reduction potentials of the model complexes are highly dependent on pH at values below 6.8, implicating proton coupling.¹²³

Biological O₂ Reduction.

The four-electron reduction of O₂ to H₂O serves as the terminal electron acceptor for both respiration and aerobic fuel cells. O₂ reduction in nature is performed primarily by the heme-copper oxidases of which cytochrome c oxidase (CcO) is

the most well-studied. In CcO, oxygen reduction occurs at the binuclear active site (BNC) which consists of a high spin heme (a_3) and a Cu coordinated to three histidine ligands (Cu_B) embedded in a hydrogen bonded network composed of amino acid residues and mobile water molecules.¹²⁴ The low reduction potential for the Cu(II) ion indicates the event is likely proton coupled.¹²⁵ One of the copper-bound histidine ligands is covalently cross-linked to a tyrosine, which likely serves as a proton or hydrogen atom donor in O_2 reduction.¹²⁶ Blue Cu oxidases have also been studied for their electrocatalytic O_2 reduction activity,¹²⁷ including bilirubin oxidase¹²⁸ and laccase.¹²⁹ The active site is composed of three Cu atoms coordinated by histidine ligands. Anaerobic reduction exhibits complex, pH-dependent behaviour for the different Cu(II) sites. The overall activity is dependent on several local carboxylate functionalities.¹³⁰

Broad reviews of molecular synthetic catalysts with O_2 reduction activity have recently been published.^{21, 131} The following examples illustrate how secondary interactions can facilitate O_2 activation, promote selective $4 e^-$ reduction to H_2O (as opposed to $2 e^-$ reduction to H_2O_2), and improve the overall catalytic activity in molecular systems.

Synthetic Catalysts for O_2 Reduction with Proton Relays.

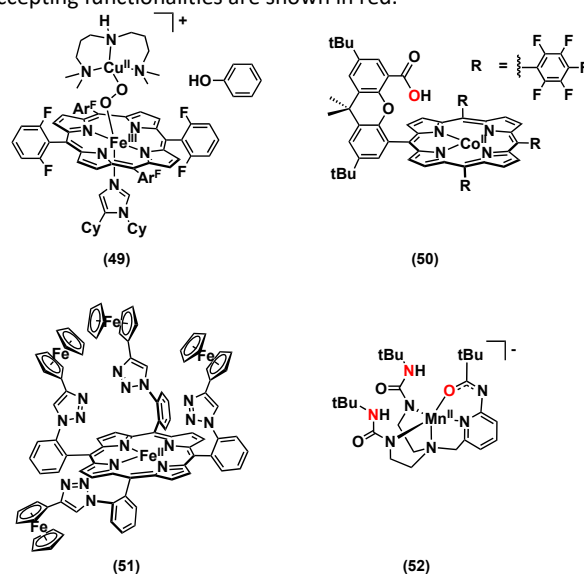
The $[Ni(P_2N_2)_2]^{2+}$ complexes most well known for hydrogen production and oxidation catalysis have also demonstrated selective stoichiometric and electrocatalytic O_2 reduction activity.¹³² Analogues that lack a pendant base or contain unprotonated bases under catalytic conditions were inactive. Although the catalyst ultimately decomposes from oxidation of the phosphine ligand, the results demonstrate the importance of a local and positioned proton source for selective O_2 reduction.

Synthetic models of the $[FeFe]$ -hydrogenase active site have also displayed some electrocatalytic activity for O_2 reduction.¹³³ The overall selectivity depends on the presence of a bridgehead N under some pH conditions. The catalyst ultimately deactivates upon oxidative degradation.

Most examples of secondary sphere modifications for O_2 activation and reduction are modified porphyrin macrocycles, which provide an oxidatively resistant platform. Early studies with Fe and Co porphyrins found the presence of a fixed hydrogen bond donor increased O_2 binding at the metal.¹³⁴ A distal carboxylic acid was also found to be critical to superoxy reduction to generate a ferric hydroperoxo in an iron porphyrin with an axial imidazole ligand.¹³⁵ Computational studies provided more details on the role of the acid.¹³⁶ Karlin, Solomon, and co-workers performed a study on the role of an intermolecular phenol on O-O bond cleavage in an Fe-Cu complex that resembles the active site of heme-copper oxidases (Chart 10, **49**).¹²⁶ Hydrogen atom transfer through a hydrogen bonded phenol effectively lowers the barrier for O-O bond homolysis, reflecting the likely role the local tyrosine residue plays in the enzymatic active site.

Catalytic reduction was explored with 'hangman' type complexes bearing rigid xanthene spacers to position a carboxylic acid over the metal (Chart 10, **50**). These studies found the combination of the pendant hydrogen bond donor

Chart 10. Molecular catalysts for O_2 reduction; proximal H^+ accepting functionalities are shown in red.



and an electron-deficient metal was key to high catalytic activity.¹³⁷ A computational analysis provided additional information about the role of the hanging group on the energy of key intermediates in the catalytic cycle.¹³⁸ A subsequent study using corrole macrocycles in the 'hangman' framework found the distal carboxylic acid functionality was critical for selective O_2 reduction.¹³⁹

Dey and co-workers have utilized porphyrins functionalized with triazoles to generate local hydrogen bonding environments.¹⁴⁰ A further modified variant includes four appended ferrocenes to the porphyrin macrocycle (Chart 10, **51**).¹⁴¹ This complex reduces O_2 over a wide pH range, likely because the local hydrogen bonded environment can provide protons at a constant acidity. Thermodynamic and kinetic studies by Dey and co-workers have also provided a comprehensive map for specific proton and electron transfer events in O_2 reduction by iron porphyrin complexes. Their analysis includes steps in which coupled proton transfer is likely, and how distal vs proximal protonation impacts selectivity.¹⁴²

A series of iron porphyrin complexes with proton donors in the secondary coordination sphere was reported by Mayer and co-workers for oxygen reduction.¹⁴³ However, a later report concluded that the apparent enhancement in activity was from an increase in driving force for O_2 activation (by more negative reduction potentials).^{12b} Computational studies found the catalytic rate is limited by O_2 activation and protonation to generate the superoxide, which correlates with the reduction potential. The lack of intramolecular proton transfer is likely due to a pK_a mismatch; the proton donors are not sufficiently acidic to donate a proton to the activated oxygen at the metal.

Borovik and co-workers have utilized tetradentate tripodal ligands that install varying hydrogen bond donors and acceptors in the secondary coordination sphere to explore their impact on O_2 activation. The number of urea functionalities, which serve as hydrogen bond donors, were found to be essential to O_2 activation in the Co complexes.¹⁴⁴ A Mn complex with the same

ligand framework containing two urea and one carboxylamido unit in the secondary coordination sphere performed selective and catalytic reduction of O₂ to H₂O (Chart 10, **52**).¹⁴⁵ The two different pendant functionalities provided unique contributions in the proposed catalytic cycle, either by stabilizing intermediates or by mediating proton delivery.

Conclusions

As illustrated through the examples above, many molecular design strategies are possible for promoting effective proton management in catalysts for multi-electron, multi-proton reactions. Secondary interactions provide different functions in promoting concerted proton transfer, adjusting the reduction potential, serving as a local proton inventory, or facilitating substrate orientation.

Although positioning, pK_a, and hydrogen bonding capabilities are clearly important considerations for optimizing secondary coordination sphere effects, questions remain on how to most effectively incorporate these elements into synthetic complexes. In order to maximize the impact of secondary interactions on catalytic activity, detailed mechanistic and kinetic studies can be used to identify catalytic barriers, such as stepwise electron-proton steps that contribute to high overpotentials or high energy transition states due to unfavourable substrate approach. These studies should include estimates or direct measurements of thermochemical values, such as pK_a for proton transfer events or reduction potentials for electron transfer events. The resulting information can inform the installation of appropriate secondary interactions to circumvent problematic catalytic steps, whether it is promoting concerted proton-electron transfer or orienting substrate. Another open question centers on the ideal degree of rigidity or flexibility of secondary interactions. Dynamic theoretical modelling can make important contributions in determining the optimal degrees of freedom. Additionally, the presence of local proton donors/acceptors in redox catalyst are known to beneficially level reduction potentials, but the different variables that contribute to the magnitude of those changes are not well understood. Lastly, the targeted use of secondary interactions to establish larger hydrogen-bonding networks for facile proton transfer or stabilize transition states is largely empirical at this point. More examples of well-defined systems accompanied by theoretical modelling would provide better guidelines for constructing productive hydrogen-bonded environments.

As mentioned in the introduction, improvement of catalytic activity upon installation of secondary functional groups does not always signify a direct role in proton management – they may instead be providing beneficial steric or electronic contributions. Replacing proton relays with functional groups with similar steric footprints can distinguish the effects of the former. Electronic contributions (through inductive effects) can be identified if there is a linear free energy relationship between the overpotential and rate. A good example of this type of analysis was performed by Mayer and coworkers on a series of O₂ reduction electrocatalysts.^{12b}

We hope the discussion and examples outline useful guidelines for improving molecular catalysts for multi-electron, multi-proton reactions through deliberate rational design.

Conflicts of interest

There are no conflicts to declare.

Acknowledgements

ZT, IPM, and JYY are supported by US Department of Energy, Office of Science, Office of Basic Energy Sciences Award DE-SC0012150 and DE-0000243266. J.Y.Y. acknowledges support as a Sloan Foundation Fellow, Canadian Institute for Advanced Research (CIFAR) Azrieli Global Scholar in the Bio-Inspired Solar Energy Program, and a Camille Dreyfus Teacher-Scholar.

Notes and references

1. C. Costentin, M. Robert and J.-M. Savéant, *Chem. Rev.*, 2010, **110**, PR1-PR40.
2. M. Sjödin, S. Styring, H. Wolpher, Y. Xu, L. Sun and L. Hammarström, *J. Am. Chem. Soc.*, 2005, **127**, 3855-3863.
3. a) D. R. Weinberg, C. J. Gagliardi, J. F. Hull, C. F. Murphy, C. A. Kent, B. C. Westlake, A. Paul, D. H. Ess, D. G. McCafferty and T. J. Meyer, *Chem. Rev.*, 2012, **112**, 4016-4093; b) A. Soudackov and S. Hammes-Schiffer, *J. Chem. Phys.*, 1999, **111**, 4672-4687.
4. a) J. L. Dempsey, J. R. Winkler and H. B. Gray, *Chem. Rev.*, 2010, **110**, 7024-7039; b) M. J. Knapp, K. Rickert and J. P. Klinman, *J. Am. Chem. Soc.*, 2002, **124**, 3865-3874; c) S. Y. Reece, J. M. Hodgkiss, J. Stubbe and D. G. Nocera, *Philos. Trans. Royal Soc. B*, 2006, **361**, 1351-1364.
5. a) S. Hammes-Schiffer, *Acc. Chem. Res.*, 2018, **51**, 1975-1983; b) S. Hammes-Schiffer, *J. Am. Chem. Soc.*, 2015, **137**, 8860-8871; c) S. Hammes-Schiffer and A. A. Stuchebrukhov, *Chem. Rev.*, 2010, **110**, 6939-6960; d) M. T. M. Koper, *Chem. Sci.*, 2013, **4**, 2710-2723; e) S. J. Mora, E. Odella, G. F. Moore, D. Gust, T. A. Moore and A. L. Moore, *Acc. Chem. Res.*, 2018, **51**, 445-453; f) S. Hammes-Schiffer, *Energy Environ. Sci.*, 2012, **5**, 7696-7703; g) S. Hammes-Schiffer, *Acc. Chem. Res.*, 2009, **42**, 1881-1889.
6. a) E. C. Gentry and R. R. Knowles, *Acc. Chem. Res.*, 2016, **49**, 1546-1556; b) A. Pannwitz and O. S. Wenger, *Chem. Commun.*, 2019, **55**, 4004-4014; c) C. J. B. Chang, J. D. K.; Chang, M. C. Y.; Baker, E. A.; Nocera, D. G., in *Electron Transfer in Chemistry*, DOI: 10.1002/9783527618248.ch41, pp. 409-461; d) J.-M. Savéant, *Annual Review of Analytical Chemistry*, 2014, **7**, 537-560; e) J. Bonin, C. Costentin, M. Robert, J.-M. Savéant and C. Tard, *Acc. Chem. Res.*, 2012, **45**, 372-381; f) J.-M. Savéant, *Energy Environ. Sci.*, 2012, **5**, 7718-7731; g) C. Costentin, M. Robert and J.-M. Savéant, *Acc. Chem. Res.*, 2010, **43**, 1019-1029; h) C. Costentin, *Chem. Rev.*, 2008, **108**, 2145-2179; i) M. Sjödin, S. Styring, B. Åkermark, L. Sun and L. Hammarström, *J. Am. Chem. Soc.*, 2000, **122**, 3932-3936; j) L. Hammarström and S. Styring, *Philos. Trans. Royal Soc. B*, 2008, **363**, 1283-1291; k) M. H. V. Huynh and T. J. Meyer, *Chem. Rev.*, 2007, **107**, 5004-5064.
7. J. M. Mayer and I. J. Rhile, *Biochimica et Biophysica Acta (BBA) - Bioenergetics*, 2004, **1655**, 51-58.
8. J. J. Warren, T. A. Tronic and J. M. Mayer, *Chem. Rev.*, 2010, **110**, 6961-7001.

9. B. Auer, L. E. Fernandez and S. Hammes-Schiffer, *J. Am. Chem. Soc.*, 2011, **133**, 8282-8292.
10. J. W. Darcy, B. Koronkiewicz, G. A. Parada and J. M. Mayer, *Acc. Chem. Res.*, 2018, **51**, 2391-2399.
11. E. R. Young, J. Rosenthal and D. G. Nocera, *Chem. Commun.*, 2008, DOI: 10.1039/B717747J, 2322-2324.
12. a) U. J. Kilgore, M. P. Stewart, M. L. Helm, W. G. Dougherty, W. S. Kassel, M. R. DuBois, D. L. DuBois and R. M. Bullock, *Inorg. Chem.*, 2011, **50**, 10908-10918; b) M. L. Pegis, B. A. McKeown, N. Kumar, K. Lang, D. J. Wasylenko, X. P. Zhang, S. Raugei and J. M. Mayer, *ACS Central Science*, 2016, **2**, 850-856.
13. I. Siewert, *Chem. – A Eur. J.*, 2015, **21**, 15078-15091.
14. W. Lubitz, H. Ogata, O. Rüdiger and E. Reijerse, *Chem. Rev.*, 2014, **114**, 4081-4148.
15. K. A. Vincent, A. Parkin and F. A. Armstrong, *Chem. Rev.*, 2007, **107**, 4366-4413.
16. M. del Barrio, M. Sensi, C. Orain, C. Baffert, S. Dementin, V. Fourmond and C. Léger, *Acc. Chem. Res.*, 2018, **51**, 769-777.
17. B. L. Greene, C.-H. Wu, P. M. McTernan, M. W. W. Adams and R. B. Dyer, *J. Am. Chem. Soc.*, 2015, **137**, 4558-4566.
18. a) Y.-C. Liu, K.-T. Chu, R.-L. Jhang, G.-H. Lee and M.-H. Chiang, *Chem. Commun.*, 2013, **49**, 4743-4745; b) R. Zaffaroni, T. B. Rauchfuss, D. L. Gray, L. De Gioia and G. Zampella, *J. Am. Chem. Soc.*, 2012, **134**, 19260-19269; c) L. De Gioia, P. Fantucci, B. Guigliarelli and P. Bertrand, *Inorg. Chem.*, 1999, **38**, 2658-2662; d) S. Niu, L. M. Thomson and M. B. Hall, *J. Am. Chem. Soc.*, 1999, **121**, 4000-4007; e) A. L. de Lacey, E. C. Hatchikian, A. Volbeda, M. Frey, J. C. Fontecilla-Camps and V. M. Fernandez, *J. Am. Chem. Soc.*, 1997, **119**, 7181-7189.
19. a) R. M. Evans, E. J. Brooke, S. A. M. Wehlin, E. Nomerotskaia, F. Sargent, S. B. Carr, S. E. V. Phillips and F. A. Armstrong, *Nat. Chem. Biol.*, 2015, **12**, 46; b) E. J. Brooke, R. M. Evans, S. T. A. Islam, G. M. Roberts, S. A. M. Wehlin, S. B. Carr, S. E. V. Phillips and F. A. Armstrong, *Biochemistry*, 2017, **56**, 132-142.
20. J.-F. Capon, F. Gloaguen, F. Y. Pétilon, P. Schollhammer and J. Talarmin, *Coord. Chem. Rev.*, 2009, **253**, 1476-1494.
21. W. Zhang, W. Lai and R. Cao, *Chem. Rev.*, 2017, **117**, 3717-3797.
22. a) A. D. Wilson, R. H. Newell, M. J. McNevin, J. T. Muckerman, M. Rakowski DuBois and D. L. DuBois, *J. Am. Chem. Soc.*, 2006, **128**, 358-366; b) M. Rakowski DuBois and D. L. DuBois, *Acc. Chem. Res.*, 2009, **42**, 1974-1982; c) M. Rakowski DuBois and D. L. DuBois, *Chem. Soc. Rev.*, 2009, **38**, 62-72; d) J. Y. Yang, R. M. Bullock, M. R. DuBois and D. L. DuBois, *MRS Bulletin*, 2011, **36**, 39-47; e) S. E. Smith, J. Y. Yang, D. L. DuBois and R. M. Bullock, *Angew. Chem.*, 2012, **124**, 3206-3209; f) W. J. Shaw, M. L. Helm and D. L. DuBois, *Biochimica et Biophysica Acta (BBA) - Bioenergetics*, 2013, **1827**, 1123-1139; g) A. Dutta, S. Lense, J. Hou, M. H. Engelhard, J. A. S. Roberts and W. J. Shaw, *J. Am. Chem. Soc.*, 2013, **135**, 18490-18496; h) D. L. DuBois, *Inorg. Chem.*, 2014, **53**, 3935-3960.
23. C. J. Curtis, A. Miedaner, W. W. Ellis and D. L. DuBois, *J. Am. Chem. Soc.*, 2002, **124**, 1918-1925.
24. C. J. Curtis, A. Miedaner, R. Ciancanelli, W. W. Ellis, B. C. Noll, M. Rakowski DuBois and D. L. DuBois, *Inorg. Chem.*, 2003, **42**, 216-227.
25. R. M. Henry, R. K. Shoemaker, D. L. DuBois and M. R. DuBois, *J. Am. Chem. Soc.*, 2006, **128**, 3002-3010.
26. K. Frazee, A. D. Wilson, A. M. Appel, M. Rakowski DuBois and D. L. DuBois, *Organometallics*, 2007, **26**, 3918-3924.
27. J. Y. Yang, R. M. Bullock, W. J. Shaw, B. Twamley, K. Frazee, M. R. DuBois and D. L. DuBois, *J. Am. Chem. Soc.*, 2009, **131**, 5935-5945.
28. S. Horvath, L. E. Fernandez, A. V. Soudackov and S. Hammes-Schiffer, *Proc. Natl. Acad. Sci.*, 2012, **109**, 15663-15668.
29. L. E. Fernandez, S. Horvath and S. Hammes-Schiffer, *The Journal of Physical Chemistry Letters*, 2013, **4**, 542-546.
30. a) L. E. Fernandez, S. Horvath and S. Hammes-Schiffer, *The Journal of Physical Chemistry C*, 2012, **116**, 3171-3180; b) S. Chen, M.-H. Ho, R. M. Bullock, D. L. DuBois, M. Dupuis, R. Rousseau and S. Raugei, *ACS Catalysis*, 2014, **4**, 229-242; c) S. Raugei, M. L. Helm, S. Hammes-Schiffer, A. M. Appel, M. O'Hagan, E. S. Wiedner and R. M. Bullock, *Inorg. Chem.*, 2016, **55**, 445-460; d) M. O'Hagan, M.-H. Ho, J. Y. Yang, A. M. Appel, M. R. DuBois, S. Raugei, W. J. Shaw, D. L. DuBois and R. M. Bullock, *J. Am. Chem. Soc.*, 2012, **134**, 19409-19424; e) A. M. Appel, D. H. Pool, M. O'Hagan, W. J. Shaw, J. Y. Yang, M. Rakowski DuBois, D. L. DuBois and R. M. Bullock, *ACS Catalysis*, 2011, **1**, 777-785; f) M. O'Hagan, W. J. Shaw, S. Raugei, S. Chen, J. Y. Yang, U. J. Kilgore, D. L. DuBois and R. M. Bullock, *J. Am. Chem. Soc.*, 2011, **133**, 14301-14312; g) S. Wiese, U. J. Kilgore, M.-H. Ho, S. Raugei, D. L. DuBois, R. M. Bullock and M. L. Helm, *ACS Catalysis*, 2013, **3**, 2527-2535; h) M.-H. Ho, R. Rousseau, J. A. S. Roberts, E. S. Wiedner, M. Dupuis, D. L. DuBois, R. M. Bullock and S. Raugei, *ACS Catalysis*, 2015, **5**, 5436-5452; i) E. S. Rountree and J. L. Dempsey, *J. Am. Chem. Soc.*, 2015, **137**, 13371-13380.
31. a) A. Dutta, D. L. DuBois, J. A. S. Roberts and W. J. Shaw, *Proc. Natl. Acad. Sci.*, 2014, **111**, 16286-16291; b) A. Jain, S. Lense, J. C. Linehan, S. Raugei, H. Cho, D. L. DuBois and W. J. Shaw, *Inorg. Chem.*, 2011, **50**, 4073-4085.
32. a) E. S. Wiedner, J. Y. Yang, W. G. Dougherty, W. S. Kassel, R. M. Bullock, M. R. DuBois and D. L. DuBois, *Organometallics*, 2010, **29**, 5390-5401; b) E. S. Wiedner, J. A. S. Roberts, W. G. Dougherty, W. S. Kassel, D. L. DuBois and R. M. Bullock, *Inorg. Chem.*, 2013, **52**, 9975-9988; c) E. S. Wiedner, A. M. Appel, D. L. DuBois and R. M. Bullock, *Inorg. Chem.*, 2013, **52**, 14391-14403; d) M. Fang, E. S. Wiedner, W. G. Dougherty, W. S. Kassel, T. Liu, D. L. DuBois and R. M. Bullock, *Organometallics*, 2014, **33**, 5820-5833.
33. a) M.-H. Ho, S. Chen, R. Rousseau, M. Dupuis, R. M. Bullock and S. Raugei, in *Applications of Molecular Modeling to Challenges in Clean Energy*, American Chemical Society, 2013, vol. 1133, ch. 6, pp. 89-111; b) U. J. Kilgore, J. A. S. Roberts, D. H. Pool, A. M. Appel, M. P. Stewart, M. R. DuBois, W. G. Dougherty, W. S. Kassel, R. M. Bullock and D. L. DuBois, *J. Am. Chem. Soc.*, 2011, **133**, 5861-5872.
34. M. Bourrez, R. Steinmetz, S. Ott, F. Gloaguen and L. Hammarström, *Nature Chemistry*, 2015, **7**, 140.
35. T. Liu, M. Guo, A. Orthaber, R. Lomoth, M. Lundberg, S. Ott and L. Hammarström, *Nature Chemistry*, 2018, **10**, 881-887.
36. D. Schilter, J. M. Camara, M. T. Huynh, S. Hammes-Schiffer and T. B. Rauchfuss, *Chem. Rev.*, 2016, **116**, 8693-8749.
37. M. E. Carroll, B. E. Barton, T. B. Rauchfuss and P. J. Carroll, *J. Am. Chem. Soc.*, 2012, **134**, 18843-18852.
38. D. J. Crouthers, J. A. Denny, R. D. Bethel, D. G. Munoz and M. Y. Darensbourg, *Organometallics*, 2014, **33**, 4747-4755.
39. M. E. Ahmed, S. Dey, M. Y. Darensbourg and A. Dey, *J. Am. Chem. Soc.*, 2018, **140**, 12457-12468.
40. S. Dey, A. Rana, S. G. Dey and A. Dey, *ACS Catalysis*, 2013, **3**, 429-436.
41. N. Elgrishi, B. D. McCarthy, E. S. Rountree and J. L. Dempsey, *ACS Catalysis*, 2016, **6**, 3644-3659.

42. a) B. H. Solis and S. Hammes-Schiffer, *Inorg. Chem.*, 2014, **53**, 6427-6443; b) B. H. Solis and S. Hammes-Schiffer, *Inorg. Chem.*, 2011, **50**, 11252-11262.
43. a) A. Bakac and J. H. Espenson, *J. Am. Chem. Soc.*, 1984, **106**, 5197-5202; b) H. B. Gjerde and J. H. Espenson, *Organometallics*, 1982, **1**, 435-440.
44. P.-A. Jacques, V. Artero, J. Pécaut and M. Fontecave, *Proc. Natl. Acad. Sci.*, 2009, **106**, 20627-20632.
45. C. C. L. McCrory, C. Uyeda and J. C. Peters, *J. Am. Chem. Soc.*, 2012, **134**, 3164-3170.
46. a) B. H. Solis, Y. Yu and S. Hammes-Schiffer, *Inorg. Chem.*, 2013, **52**, 6994-6999; b) A. Bhattacharjee, E. S. Andreiadis, M. Chavarot-Kerlidou, M. Fontecave, M. J. Field and V. Artero, *Chemistry – A European Journal*, 2013, **19**, 15166-15174.
47. A. Gerli, M. Sabat and L. G. Marzilli, *J. Am. Chem. Soc.*, 1992, **114**, 6711-6718.
48. B. Probst, M. Guttentag, A. Rodenberg, P. Hamm and R. Alberto, *Inorg. Chem.*, 2011, **50**, 3404-3412.
49. P. Huo, C. Uyeda, J. D. Goodpaster, J. C. Peters and T. F. Miller, *ACS Catalysis*, 2016, **6**, 6114-6123.
50. a) C. H. Lee, D. K. Dogutan and D. G. Nocera, *J. Am. Chem. Soc.*, 2011, **133**, 8775-8777; b) M. M. Roubelakis, D. K. Bediako, D. K. Dogutan and D. G. Nocera, *Energy Environ. Sci.*, 2012, **5**, 7737-7740; c) B. H. Solis, A. G. Maher, T. Honda, D. C. Powers, D. G. Nocera and S. Hammes-Schiffer, *ACS Catalysis*, 2014, **4**, 4516-4526.
51. D. K. Bediako, B. H. Solis, D. K. Dogutan, M. M. Roubelakis, A. G. Maher, C. H. Lee, M. B. Chambers, S. Hammes-Schiffer and D. G. Nocera, *Proc. Natl. Acad. Sci.*, 2014, **111**, 15001-15006.
52. L. Chen, M. Wang, K. Han, P. Zhang, F. Gloaguen and L. Sun, *Energy Environ. Sci.*, 2014, **7**, 329-334.
53. Y.-Q. Zhang and R.-Z. Liao, *Phys. Chem. Chem. Phys.*, 2017, **19**, 32589-32596.
54. G. K. Rao, M. P. Jamshidi, J. I. G. Dawkins, W. Pell, I. Korobkov and D. Richeson, *Dalton Trans.*, 2017, **46**, 6518-6522.
55. a) Z. Han, L. Shen, W. W. Brennessel, P. L. Holland and R. Eisenberg, *J. Am. Chem. Soc.*, 2013, **135**, 14659-14669; b) Z. Han, W. R. McNamara, M.-S. Eum, P. L. Holland and R. Eisenberg, *Angewandte Chemie International Edition*, 2012, **51**, 1667-1670.
56. a) S. Li and M. B. Hall, *Inorg. Chem.*, 2001, **40**, 18-24; b) G. A. N. Felton, C. A. Mebi, B. J. Petro, A. K. Vannucci, D. H. Evans, R. S. Glass and D. L. Lichtenberger, *J. Organomet. Chem.*, 2009, **694**, 2681-2699.
57. a) Q. Tang and D.-e. Jiang, *ACS Catalysis*, 2016, **6**, 4953-4961; b) T. Liao, Z. Sun, C. Sun, S. X. Dou and D. J. Searles, *Scientific Reports*, 2014, **4**, 6256; c) J. Wang, J. Liu, B. Zhang, X. Ji, K. Xu, C. Chen, L. Miao and J. Jiang, *Phys. Chem. Chem. Phys.*, 2017, **19**, 10125-10132.
58. H. I. Karunadasa, E. Montalvo, Y. Sun, M. Majda, J. R. Long and C. J. Chang, *Science*, 2012, **335**, 698-702.
59. R. Schaugaard, C. C. Jarrold and K. Raghavachari, *Inorg. Chem.*, 2018, **57**, 9167-9174.
60. K. Weber, T. Krämer, H. S. Shafaat, T. Weyhermüller, E. Bill, M. van Gastel, F. Neese and W. Lubitz, *J. Am. Chem. Soc.*, 2012, **134**, 20745-20755.
61. a) P. Ghosh, S. Ding, R. B. Chupik, M. Quiroz, C.-H. Hsieh, N. Bhuvanesh, M. B. Hall and M. Y. Darensbourg, *Chem. Sci.*, 2017, **8**, 8291-8300; b) P. Ghosh, M. Quiroz, N. Wang, N. Bhuvanesh and M. Y. Darensbourg, *Dalton Trans.*, 2017, **46**, 5617-5624; c) S. Ding, P. Ghosh, A. M. Lunsford, N. Wang, N. Bhuvanesh, M. B. Hall and M. Y. Darensbourg, *J. Am. Chem. Soc.*, 2016, **138**, 12920-12927.
62. P. Surawatanawong, J. W. Tye, M. Y. Darensbourg and M. B. Hall, *Dalton Trans.*, 2010, **39**, 3093-3104.
63. a) W. R. McNamara, Z. Han, P. J. Alperin, W. W. Brennessel, P. L. Holland and R. Eisenberg, *J. Am. Chem. Soc.*, 2011, **133**, 15368-15371; b) W. R. McNamara, Z. Han, C.-J. Yin, W. W. Brennessel, P. L. Holland and R. Eisenberg, *Proc. Natl. Acad. Sci.*, 2012, **109**, 15594-15599.
64. B. H. Solis and S. Hammes-Schiffer, *J. Am. Chem. Soc.*, 2012, **134**, 15253-15256.
65. C. S. Letko, J. A. Panetier, M. Head-Gordon and T. D. Tilley, *J. Am. Chem. Soc.*, 2014, **136**, 9364-9376.
66. T. Fogeron, J.-P. Porcher, M. Gomez-Mingot, T. K. Todorova, L.-M. Chamoreau, C. Mellot-Draznieks, Y. Li and M. Fontecave, *Dalton Trans.*, 2016, **45**, 14754-14763.
67. Y. Aimoto, K. Koshiba, K. Yamauchi and K. Sakai, *Chem. Commun.*, 2018, **54**, 12820-12823.
68. C. P. Yap, K. Hou, A. A. Bengali and W. Y. Fan, *Inorg. Chem.*, 2017, **56**, 10926-10931.
69. A. Zarkadoulas, M. J. Field, C. Papatriantafyllopoulou, J. Fize, V. Artero and C. A. Mitsopoulou, *Inorg. Chem.*, 2016, **55**, 432-444.
70. M. Gomez-Mingot, J.-P. Porcher, T. K. Todorova, T. Fogeron, C. Mellot-Draznieks, Y. Li and M. Fontecave, *The Journal of Physical Chemistry B*, 2015, **119**, 13524-13533.
71. a) J. M. Camara and T. B. Rauchfuss, *J. Am. Chem. Soc.*, 2011, **133**, 8098-8101; b) J. M. Camara and T. B. Rauchfuss, *Nature Chemistry*, 2011, **4**, 26.
72. J. Y. Yang, S. Chen, W. G. Dougherty, W. S. Kassel, R. M. Bullock, D. L. DuBois, S. Raugei, R. Rousseau, M. Dupuis and M. R. DuBois, *Chem. Commun.*, 2010, **46**, 8618-8620.
73. J. Y. Yang, S. E. Smith, T. Liu, W. G. Dougherty, W. A. Hoffert, W. S. Kassel, M. R. DuBois, D. L. DuBois and R. M. Bullock, *J. Am. Chem. Soc.*, 2013, **135**, 9700-9712.
74. R. M. Stolley, J. M. Darmon and M. L. Helm, *Chem. Commun.*, 2014, **50**, 3681-3684.
75. P. Das, M.-H. Ho, M. O'Hagan, W. J. Shaw, R. Morris Bullock, S. Raugei and M. L. Helm, *Dalton Trans.*, 2014, **43**, 2744-2754.
76. a) T. Liu, Q. Liao, M. O'Hagan, E. B. Hulley, D. L. DuBois and R. M. Bullock, *Organometallics*, 2015, **34**, 2747-2764; b) T. Liu, S. Chen, M. J. O'Hagan, M. Rakowski DuBois, R. M. Bullock and D. L. DuBois, *J. Am. Chem. Soc.*, 2012, **134**, 6257-6272; c) T. Liu, D. L. DuBois and R. M. Bullock, *Nature Chemistry*, 2013, **5**, 228.
77. a) E. B. Hulley, N. Kumar, S. Raugei and R. M. Bullock, *ACS Catalysis*, 2015, **5**, 6838-6847; b) E. B. Hulley, M. L. Helm and R. M. Bullock, *Chem. Sci.*, 2014, **5**, 4729-4741.
78. T. Liu, M. R. DuBois, D. L. DuBois and R. M. Bullock, *Energy Environ. Sci.*, 2014, **7**, 3630-3639.
79. a) M. Alfonso-Prieto, X. Biarnés, P. Vidossich and C. Rovira, *J. Am. Chem. Soc.*, 2009, **131**, 11751-11761; b) P. Nicholls, I. Fita and P. C. Loewen, in *Adv. Inorg. Chem.*, Academic Press, 2000, vol. 51, pp. 51-106.
80. S.-i. Ozaki, M. P. Roach, T. Matsui and Y. Watanabe, *Acc. Chem. Res.*, 2001, **34**, 818-825.
81. C. Costentin, V. Hajj, M. Robert, J.-M. Savéant and C. Tard, *Proc. Natl. Acad. Sci.*, 2011, **108**, 8559-8564.
82. a) C.-Y. Yeh, C. J. Chang and D. G. Nocera, *J. Am. Chem. Soc.*, 2001, **123**, 1513-1514; b) C. J. Chang, L. L. Chng and D. G. Nocera, *J. Am. Chem. Soc.*, 2003, **125**, 1866-1876.
83. a) S.-Y. Liu, J. D. Soper, J. Y. Yang, E. V. Rybak-Akimova and D. G. Nocera, *Inorg. Chem.*, 2006, **45**, 7572-7574; b) J. Y. Yang, J. Bachmann and D. G. Nocera, *The Journal of Organic Chemistry*, 2006, **71**, 8706-8714; c) J. Y. Yang and D. G. Nocera, *J. Am. Chem. Soc.*, 2007, **129**, 8192-8198; d) J. Y. Yang and D. G. Nocera,

- Tetrahedron Lett.*, 2008, **49**, 4796-4798; e) J. Y. Yang, S.-Y. Liu, I. V. Korendovych, E. V. Rybak-Akimova and D. G. Nocera, *ChemSusChem*, 2008, **1**, 941-949.
84. a) Y. G. Abashkin and S. K. Burt, *Inorg. Chem.*, 2005, **44**, 1425-1432; b) Y. G. Abashkin and S. K. Burt, *The Journal of Physical Chemistry B*, 2004, **108**, 2708-2711.
85. S. R. Doctrow, K. Huffman, C. B. Marcus, G. Tocco, E. Malfroy, C. A. Adinolfi, H. Kruk, K. Baker, N. Lazarowich, J. Mascarenhas and B. Malfroy, *J. Med. Chem.*, 2002, **45**, 4549-4558.
86. a) Y. Umena, K. Kawakami, J.-R. Shen and N. Kamiya, *Nature*, 2011, **473**, 55; b) J. Kern, R. Chatterjee, I. D. Young, F. D. Fuller, L. Lassalle, M. Ibrahim, S. Gul, T. Fransson, A. S. Brewster, R. Alonso-Mori, R. Hussein, M. Zhang, L. Douthit, C. de Lichtenberg, M. H. Cheah, D. Shevela, J. Wersig, I. Seuffert, D. Sokaras, E. Pastor, C. Weninger, T. Kroll, R. G. Sierra, P. Aller, A. Butryn, A. M. Orville, M. Liang, A. Batyuk, J. E. Koglin, S. Carbajo, S. Boutet, N. W. Moriarty, J. M. Holton, H. Dobbek, P. D. Adams, U. Bergmann, N. K. Sauter, A. Zouni, J. Messinger, J. Yano and V. K. Yachandra, *Nature*, 2018, **563**, 421-425; c) B. A. Barry, U. Brahmachari and Z. Guo, *Acc. Chem. Res.*, 2017, **50**, 1937-1945.
87. L. Vogt, D. J. Vinyard, S. Khan and G. W. Brudvig, *Curr. Opin. Chem. Biol.*, 2015, **25**, 152-158.
88. a) C. Tommos and G. T. Babcock, *Biochimica et Biophysica Acta (BBA) - Bioenergetics*, 2000, **1458**, 199-219; b) J. D. Megiatto Jr, D. D. Méndez-Hernández, M. E. Tejada-Ferrari, A.-L. Teillout, M. J. Llansola-Portolés, G. Kodis, O. G. Poluektov, T. Rajh, V. Mujica, T. L. Groy, D. Gust, T. A. Moore and A. L. Moore, *Nature Chemistry*, 2014, **6**, 423.
89. a) R. Gilson and M. C. Durrant, *Dalton Transactions*, 2009, DOI: 10.1039/B911593E, 10223-10230; b) M. Amin, L. Vogt, S. Vassiliev, I. Rivalta, M. M. Sultan, D. Bruce, G. W. Brudvig, V. S. Batista and M. R. Gunner, *The Journal of Physical Chemistry B*, 2013, **117**, 6217-6226.
90. a) D. J. Vinyard and G. W. Brudvig, *Annu. Rev. Phys. Chem.*, 2017, **68**, 101-106; b) G. W. Brudvig, a. W. F. Beck and J. C. Paula, *Annual Review of Biophysics and Biophysical Chemistry*, 1989, **18**, 25-46; c) N. Cox, D. A. Pantazis, F. Neese and W. Lubitz, *Acc. Chem. Res.*, 2013, **46**, 1588-1596; d) H. Bao, P. L. Dilbeck and R. L. Burnap, *Photosynth. Res.*, 2013, **116**, 215-229; e) A. Klaus, M. Haumann and H. Dau, *Proc. Natl. Acad. Sci.*, 2012, **109**, 16035-16040; f) L. I. Krishtalik, *Bioelectrochem. Bioenerg.*, 1990, **23**, 249-263; g) C. W. Hoganson and G. T. Babcock, *Science*, 1997, **277**, 1953-1956.
91. a) M. J. Baldwin and V. L. Pecoraro, *J. Am. Chem. Soc.*, 1996, **118**, 11325-11326; b) B. Lassalle-Kaiser, C. Hureau, D. A. Pantazis, Y. Pushkar, R. Guillot, V. K. Yachandra, J. Yano, F. Neese and E. Anxolabehere-Mallart, *Energy Environ. Sci.*, 2010, **3**, 924-938; c) H. H. Thorp, J. E. Sarneski, G. W. Brudvig and R. H. Crabtree, *J. Am. Chem. Soc.*, 1989, **111**, 9249-9250; d) R. Manchanda, H. H. Thorp, G. W. Brudvig and R. H. Crabtree, *Inorg. Chem.*, 1991, **30**, 494-497; e) M. J. Baldwin, A. Gelasco and V. L. Pecoraro, *Photosynth. Res.*, 1993, **38**, 303-308; f) K. J. Takeuchi, G. J. Samuels, S. W. Gersten, J. A. Gilbert and T. J. Meyer, *Inorg. Chem.*, 1983, **22**, 1407-1409; g) J. C. Dobson, K. J. Takeuchi, D. W. Pipes, D. A. Geselowitz and T. J. Meyer, *Inorg. Chem.*, 1986, **25**, 2357-2365; h) J. C. Dobson and T. J. Meyer, *Inorg. Chem.*, 1988, **27**, 3283-3291; i) D. W. Pipes and T. J. Meyer, *Inorg. Chem.*, 1986, **25**, 3256-3262.
92. M. D. Kärkäs, O. Verho, E. V. Johnston and B. Åkermark, *Chem. Rev.*, 2014, **114**, 11863-12001.
93. Z. Chen, J. J. Concepcion, X. Hu, W. Yang, P. G. Hoertz and T. J. Meyer, *Proc. Natl. Acad. Sci.*, 2010, **107**, 7225-7229.
94. a) J. D. Blakemore, R. H. Crabtree and G. W. Brudvig, *Chem. Rev.*, 2015, **115**, 12974-13005; b) J. Li, R. Güttinger, R. Moré, F. Song, W. Wan and G. R. Patzke, *Chem. Soc. Rev.*, 2017, **46**, 6124-6147.
95. S. W. Gersten, G. J. Samuels and T. J. Meyer, *J. Am. Chem. Soc.*, 1982, **104**, 4029-4030.
96. F. Liu, J. J. Concepcion, J. W. Jurss, T. Cardolaccia, J. L. Templeton and T. J. Meyer, *Inorg. Chem.*, 2008, **47**, 1727-1752.
97. a) J. J. Concepcion, J. W. Jurss, J. L. Templeton and T. J. Meyer, *J. Am. Chem. Soc.*, 2008, **130**, 16462-16463; b) J. J. Concepcion, J. W. Jurss, M. R. Norris, Z. Chen, J. L. Templeton and T. J. Meyer, *Inorg. Chem.*, 2010, **49**, 1277-1279; c) Z. Chen, J. J. Concepcion, J. W. Jurss and T. J. Meyer, *J. Am. Chem. Soc.*, 2009, **131**, 15580-15581.
98. J. L. Fillol, Z. Codolà, I. Garcia-Bosch, L. Gómez, J. J. Pla and M. Costas, *Nature Chemistry*, 2011, **3**, 807.
99. F. Acuña-Parés, Z. Codolà, M. Costas, J. M. Luis and J. Lloret-Fillol, *Chemistry – A European Journal*, 2014, **20**, 5696-5707.
100. T. Ishizuka, A. Watanabe, H. Kotani, D. Hong, K. Satonaka, T. Wada, Y. Shiota, K. Yoshizawa, K. Ohara, K. Yamaguchi, S. Kato, S. Fukuzumi and T. Kojima, *Inorg. Chem.*, 2016, **55**, 1154-1164.
101. M.-T. Zhang, Z. Chen, P. Kang and T. J. Meyer, *J. Am. Chem. Soc.*, 2013, **135**, 2048-2051.
102. W. A. Hoffert, M. T. Mock, A. M. Appel and J. Y. Yang, *Eur. J. Inorg. Chem.*, 2013, **2013**, 3846-3857.
103. J. F. Khosrowabadi Kotyk, C. M. Hanna, R. L. Combs, J. W. Ziller and J. Y. Yang, *Chem. Sci.*, 2018, **9**, 2750-2755.
104. D. K. Dogutan, R. McGuire and D. G. Nocera, *J. Am. Chem. Soc.*, 2011, **133**, 9178-9180.
105. M. Z. Ertem and C. J. Cramer, *Dalton Trans.*, 2012, **41**, 12213-12219.
106. W. Lai, R. Cao, G. Dong, S. Shaik, J. Yao and H. Chen, *The Journal of Physical Chemistry Letters*, 2012, **3**, 2315-2319.
107. H. Lei, A. Han, F. Li, M. Zhang, Y. Han, P. Du, W. Lai and R. Cao, *Phys. Chem. Chem. Phys.*, 2014, **16**, 1883-1893.
108. H. Sun, Y. Han, H. Lei, M. Chen and R. Cao, *Chem. Commun.*, 2017, **53**, 6195-6198.
109. W. A. A. Arafat, M. D. Kärkäs, B.-L. Lee, T. Åkermark, R.-Z. Liao, H.-M. Berends, J. Messinger, P. E. M. Siegbahn and B. Åkermark, *Phys. Chem. Chem. Phys.*, 2014, **16**, 11950-11964.
110. T. Zhang, C. Wang, S. Liu, J.-L. Wang and W. Lin, *J. Am. Chem. Soc.*, 2014, **136**, 273-281.
111. G. Maayan, N. Gluz and G. Christou, *Nature Catalysis*, 2018, **1**, 48-54.
112. T. Ghosh and G. Maayan, *Angewandte Chemie International Edition*, 2019, **58**, 2785-2790.
113. X. Sala, S. Maji, R. Bofill, J. García-Antón, L. Escriche and A. Llobet, *Acc. Chem. Res.*, 2014, **47**, 504-516.
114. L. Vigara, M. Z. Ertem, N. Planas, F. Bozoglian, N. Leidel, H. Dau, M. Haumann, L. Gagliardi, C. J. Cramer and A. Llobet, *Chem. Sci.*, 2012, **3**, 2576-2586.
115. Z. Deng, H.-W. Tseng, R. Zong, D. Wang and R. Thummel, *Inorg. Chem.*, 2008, **47**, 1835-1848.
116. R. Zong and R. P. Thummel, *J. Am. Chem. Soc.*, 2005, **127**, 12802-12803.
117. J. L. Boyer, D. E. Polyansky, D. J. Szalda, R. Zong, R. P. Thummel and E. Fujita, *Angew. Chem.*, 2011, **123**, 12808-12812.
118. a) L. Duan, A. Fischer, Y. Xu and L. Sun, *J. Am. Chem. Soc.*, 2009, **131**, 10397-10399; b) L. Duan, F. Bozoglian, S. Mandal, B. Stewart, T. Privalov, A. Llobet and L. Sun, *Nature Chemistry*, 2012, **4**, 418; c) L. Wang, L. Duan, B. Stewart, M. Pu, J. Liu, T. Privalov and L. Sun, *J. Am. Chem. Soc.*, 2012, **134**, 18868-18880.

119. D. W. Shaffer, Y. Xie, D. J. Szalda and J. J. Concepcion, *J. Am. Chem. Soc.*, 2017, **139**, 15347-15355.
120. F. Chen, N. Wang, H. Lei, D. Guo, H. Liu, Z. Zhang, W. Zhang, W. Lai and R. Cao, *Inorg. Chem.*, 2017, **56**, 13368-13375.
121. X.-J. Su, M. Gao, L. Jiao, R.-Z. Liao, P. E. M. Siegbahn, J.-P. Cheng and M.-T. Zhang, *Angewandte Chemie International Edition*, 2015, **54**, 4909-4914.
122. a) T. K. Michaelos, D. Y. Shopov, S. B. Sinha, L. S. Sharninghausen, K. J. Fisher, H. M. C. Lant, R. H. Crabtree and G. W. Brudvig, *Acc. Chem. Res.*, 2017, **50**, 952-959; b) L. S. Sharninghausen, S. B. Sinha, D. Y. Shopov, B. Choi, B. Q. Mercado, X. Roy, D. Balcells, G. W. Brudvig and R. H. Crabtree, *J. Am. Chem. Soc.*, 2016, **138**, 15917-15926.
123. D. Y. Shopov, B. Rudshiteyn, J. Campos, V. S. Batista, R. H. Crabtree and G. W. Brudvig, *J. Am. Chem. Soc.*, 2015, **137**, 7243-7250.
124. a) S. Ferguson-Miller and G. T. Babcock, *Chem. Rev.*, 1996, **96**, 2889-2908; b) S. Yoshikawa and A. Shimada, *Chem. Rev.*, 2015, **115**, 1936-1989.
125. M. R. A. Blomberg, *Biochemistry*, 2016, **55**, 489-500.
126. A. W. Schaefer, M. T. Kieber-Emmons, S. M. Adam, K. D. Karlin and E. I. Solomon, *J. Am. Chem. Soc.*, 2017, **139**, 7958-7973.
127. J. A. Cracknell, K. A. Vincent and F. A. Armstrong, *Chem. Rev.*, 2008, **108**, 2439-2461.
128. N. Mano, J. L. Fernandez, Y. Kim, W. Shin, A. J. Bard and A. Heller, *J. Am. Chem. Soc.*, 2003, **125**, 15290-15291.
129. a) S. C. Barton, H.-H. Kim, G. Binyamin, Y. Zhang and A. Heller, *The Journal of Physical Chemistry B*, 2001, **105**, 11917-11921; b) N. Mano, V. Soukharev and A. Heller, *The Journal of Physical Chemistry B*, 2006, **110**, 11180-11187; c) C. F. Blanford, R. S. Heath and F. A. Armstrong, *Chem. Commun.*, 2007, DOI: 10.1039/B703114A, 1710-1712; d) C. F. Blanford, C. E. Foster, R. S. Heath and F. A. Armstrong, *Faraday Discuss.*, 2009, **140**, 319-335; e) M. S. Thorum, C. A. Anderson, J. J. Hatch, A. S. Campbell, N. M. Marshall, S. C. Zimmerman, Y. Lu and A. A. Gewirth, *The Journal of Physical Chemistry Letters*, 2010, **1**, 2251-2254.
130. S. M. Jones and E. I. Solomon, *Cell. Mol. Life Sci.*, 2015, **72**, 869-883.
131. M. L. Pegis, C. F. Wise, D. J. Martin and J. M. Mayer, *Chem. Rev.*, 2018, **118**, 2340-2391.
132. J. Y. Yang, R. M. Bullock, W. G. Dougherty, W. S. Kassel, B. Twamley, D. L. DuBois and M. Rakowski DuBois, *Dalton Trans.*, 2010, **39**, 3001-3010.
133. S. Dey, A. Rana, D. Crouthers, B. Mondal, P. K. Das, M. Y. Darensbourg and A. Dey, *J. Am. Chem. Soc.*, 2014, **136**, 8847-8850.
134. a) G. E. Wuenschell, C. Tetreau, D. Lavalette and C. A. Reed, *J. Am. Chem. Soc.*, 1992, **114**, 3346-3355; b) C. K. Chang, Y. Liang, G. Aviles and S.-M. Peng, *J. Am. Chem. Soc.*, 1995, **117**, 4191-4192.
135. P. Nagaraju, T. Ohta, J.-G. Liu, T. Ogura and Y. Naruta, *Chem. Commun.*, 2016, **52**, 7213-7216.
136. T. Ohta, P. Nagaraju, J.-G. Liu, T. Ogura and Y. Naruta, *JBIC Journal of Biological Inorganic Chemistry*, 2016, **21**, 745-755.
137. R. McGuire Jr, D. K. Dogutan, T. S. Teets, J. Suntivich, Y. Shao-Horn and D. G. Nocera, *Chem. Sci.*, 2010, **1**, 411-414.
138. J. D. Baran, H. Grönbeck and A. Hellman, *J. Am. Chem. Soc.*, 2014, **136**, 1320-1326.
139. D. K. Dogutan, S. A. Stoian, R. McGuire, M. Schwalbe, T. S. Teets and D. G. Nocera, *J. Am. Chem. Soc.*, 2011, **133**, 131-140.
140. K. Mittra, S. Chatterjee, S. Samanta, K. Sengupta, H. Bhattacharjee and A. Dey, *Chem. Commun.*, 2012, **48**, 10535-10537.
141. K. Mittra, S. Chatterjee, S. Samanta and A. Dey, *Inorg. Chem.*, 2013, **52**, 14317-14325.
142. S. Chatterjee, K. Sengupta, B. Mondal, S. Dey and A. Dey, *Acc. Chem. Res.*, 2017, **50**, 1744-1753.
143. a) C. T. Carver, B. D. Matson and J. M. Mayer, *J. Am. Chem. Soc.*, 2012, **134**, 5444-5447; b) B. D. Matson, C. T. Carver, A. Von Ruden, J. Y. Yang, S. Raugi and J. M. Mayer, *Chem. Commun.*, 2012, **48**, 11100-11102.
144. R. L. Z. Lucas, M. K.; Mukherjee, J.; Sorrell, T. N.; Powell, D. R.; Borovik, A. S., *J. Am. Chem. Soc.*, 2007, **128**, 15476-15489.
145. R. L. Shook, S. M. Peterson, J. Greaves, C. Moore, A. L. Rheingold and A. S. Borovik, *J. Am. Chem. Soc.*, 2011, **133**, 5810-5817.